Marine Geology 472 (2024) 107308

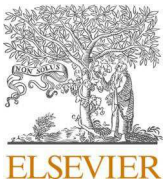

Contents lists available at ScienceDirect

Marine Geology

journal homepage: www.elsevier.com/locate/margo

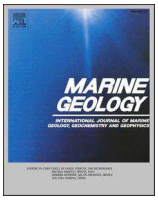

Submarine morphology of Pantelleria volcano: The interplay between volcanic and erosive-depositional processes modulated by sea-level fluctuations.

Daniele Casalbore [a,b,*], Claudia Romagnoli [b,c], Marilena Calarco [d], Alessandro Bosman [b], Eleonora Martorelli [b], Francesco Latino Chiocci [a,b]

[a] Sapienza, University of Rome, Italy
[b] CNR-IGAG, Italy
[c] University of Bologna, Italy
[d] RINA Consulting S.P.A., Italy

ARTICLE INFO

Editor: Michele Rebesco

Keywords:
Seafloor morphology
Volcano-tectonic interaction
Lava flows
Insular shelf
Mass-wasting

ABSTRACT

High-resolution multibeam data integrated with seismic reflection profiles are used to identify and characterize the main primary volcanic and erosive-depositional features along the submarine part (about the 80%) of the active Pantelleria volcano located in the Sicily Channel. Volcanic features include lava flows, cones and elongated ridges. Lava flows are mainly recognized over the insular shelf, while volcanic cones and ridges are mostly concentrated along the steep submarine flanks, especially along the wider SE and NW ones. A strong volcano-tectonic interaction is envisaged for their formation, as indicated by their preferential elongation or alignment along the (main) SE-NW and (secondary) SW-NE directions that have controlled the evolution of the whole volcanic edifice. Erosive-depositional features mainly include small-scale landslide scars and narrow gullies affecting the edge of the insular shelf and overlying submarine depositional terraces. Gullies sometimes merge downslope in larger channels, whose formation is primarily controlled by the distribution of volcanic features and/or shelf sectors characterized by different age or lithologies. Based on the marked morphological differences between the different flanks of the Pantelleria volcano, we infer an overall migration of the volcanic activity from SE to NW over time. This migration is apparently in contrast with the presence of a much wider but shallower NW insular shelf with respect to the SE one. This anomaly can be explained through a two-stage model, with the formation, in the NW sector, of a polygenic shelf rejuvenated by volcanic progradation during the last eustatic hemicycle. The different depths of the insular shelf edge around the island also provide insights on vertical deformations that affected the Pantelleria volcano during the Late-Quaternary.

1. Introduction

The study of the submarine part of insular volcanoes has exponentially increased in the last decades through recent advances in seafloor imagery systems and seismic techniques, which allow identifying the main volcanic, tectonic and sedimentary processes and their interactions (e.g., Mitchell et al., 2002; Boudon et al., 2007; Romagnoli et al., 2013; Casalbore, 2018; Quartau et al., 2018; Tzevahirtzian et al., 2021). These studies have mainly focused on active volcanoes, where volcanic eruptions, landslides processes and related tsunamis can represent a real geohazard for the coastal communities, as recently testified by the 2018 tsunamigenic collapse of Anak Krakatau with 437 fatalities (Hunt et al., 2021) or the 2022 catastrophic at Hunga Tonga-Hunga Ha'apa tsunamigenic eruption (Lynett et al., 2022; Clare et al., 2023). At more local scale, submarine eruptions in shallow or intermediate waters can represent a threat for offshore infrastructures and surrounding coastal communities, as testified by the 2010 eruption at South Sarigan Seamount (Embley et al., 2014), the 2011–2012 eruption at El Hierro (Carracedo et al., 2015), the 2014–2015 eruption at Hunga Tonga-Hunga Ha'apai (Colombier et al., 2018), and the 2016–2017 eruption at Bogoso (Coombs et al., 2019).

In this study, we analyse for the first time the detailed submarine

* Corresponding author at: Sapienza, University of Rome, Italy.
E-mail address: daniele.casalbore@uniroma1.it (D. Casalbore).

https://doi.org/10.1016/j.margeo.2024.107308
Received 29 December 2023; Received in revised form 9 April 2024; Accepted 10 May 2024
Available online 17 May 2024

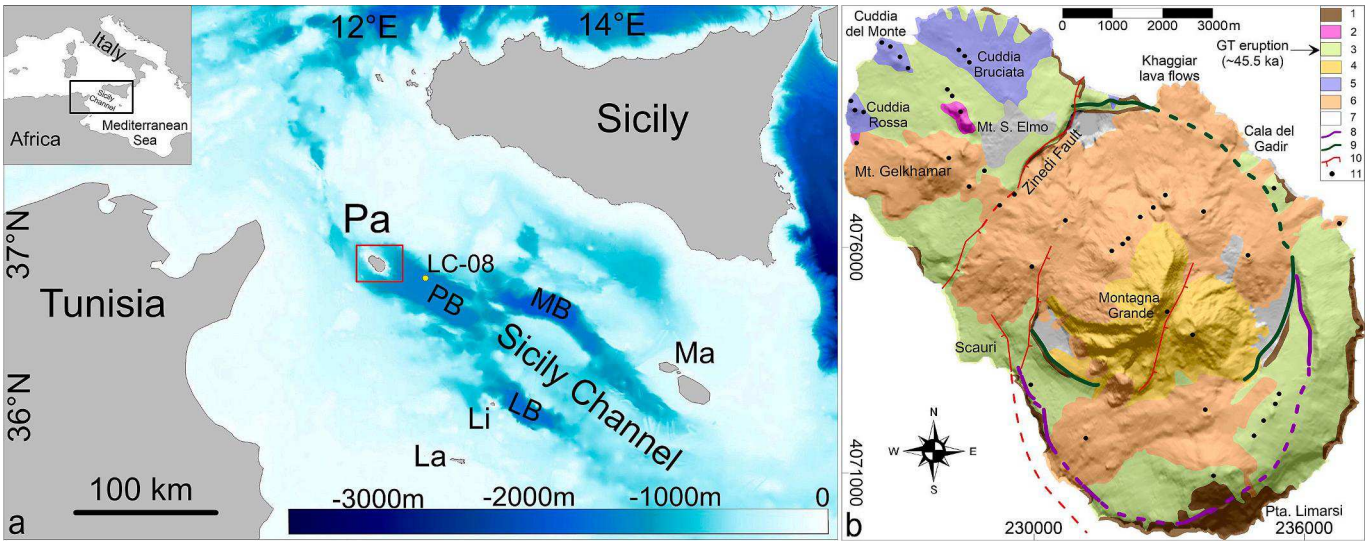

Fig. 1. a) General bathy-morphological setting of the Sicily Channel (data from Emodnet bathymetry, https://emodnet.ec.europa.eu/en/bathymetry), with the indication of the main basins (PB: Pantelleria Basin, MB: Malta Basin, LB: Linosa Basin), islands (Pa: Pantelleria; Li: Linosa; La: Lampedusa; Ma: Malta), study area (red box) and core LC-08 (yellow circle, from Reeder et al., 2002). b) Simplified geological map of Pantelleria island (modified from Rotolo et al., 2017) draped over the island topography. 1 Pre-Green Tuff pantellerites; 2 Pre-Green Tuff basalts; 3 Green Tuff; 4 Post-Green Tuff trachyte lavas and domes; 5 Post-Green Tuff basalts; 6 Post-Green Tuff pantelleritic pumice falls and lava flows; 7 Alluvium and fill; 8 La Vecchia caldera rim; 9 Cinque Denti caldera rim; 10 Faults; 11 Principal eruptive vents. (For interpretation of the references to colour in this figure legend, the reader is referred to the web version of this article.)

morphology of the Pantelleria volcano located in the Sicily Channel between Sicily and Tunisia (Fig. 1a; Boccaletti et al., 1987). The area is generally considered to represent an example of intraplate "passive", NW-trending rift, where volcanism is a consequence of tensional stresses on the lithosphere due to the regional stress field in an anorogenic setting (Civile et al., 2010). Recent studies have evidenced a more complex tectonic evolution of the area, with the superimposition of extensional and contractional phases (Maiorana et al., 2023 and reference therein).

The Pantelleria volcano is still active, and its last known eruption occurred in 1891 at intermediate water depths, being characterized by the emission of peculiar products known as floating "lava balloons" (Conte et al., 2014 and reference therein), similarly to what was observed more recently during the 1998–2001 Serreta eruption (Gaspar et al., 2003; Casas et al., 2018) and the 2011–2012 El Hierro eruption (Somoza et al., 2017). At present, the island has an active diffuse hydrothermal activity with steaming ground, mofettes and hot springs, particularly in the intra- and peri-caldera zones (Fulignati et al., 1997).

Based on the integration of geophysical data (multibeam data with seismic reflections profiles), the aim of this paper is twofold: (1) to show the interplay between volcanic, tectonic and erosive-depositional processes, modulated by sea-level fluctuations, in shaping the submarine morphology of the Pantelleria edifice; (2) to shed light on the morpho-structural evolution of this volcano, including new insights on vertical deformations occurred during the Late-Quaternary, provided by marine geomorphic markers.

2. Geological setting

Pantelleria Island has an elevation of 836 m above sea level (culminating in Montagna Grande, Fig. 1b) and covers an area of approximately 83 km^2, representing the summit of a large volcanic edifice that rises approximately 2000 m from the surrounding seafloor. The volcanic edifice lies in the northwestern portion of the Pantelleria Basin (PB in Fig. 1a), a tectonic depression approximately 90 km long and 30–40 km wide. The PB is bounded by NW–SE trending normal faults and is partially filled by over 1000 m of lower Pliocene–Quaternary deposits (Civile et al., 2010). The PB, together with the Malta and Linosa basins (MB and LB in Fig. 1a), is one the most striking and deepest (water depth down to 1700 m) morpho-tectonic features of the Sicilian Channel Rift Zone (Finetti, 1984) developed since the Early Pliocene (Civile et al., 2008). The PB evolution has been divided in two main tectonic phases (Civile et al., 2010): a first lithospheric-scale continental rifting phase (Early Pliocene), during which the whole tectonic depression was formed, and a successive phase (Late Pliocene–Pleistocene) characterized by the development of volcanism related to anorogenic magma, with mostly alkaline to peralkaline affinity (Calanchi et al., 1989). According to the evidence shown in seismic profiles, the magmatic activity in the PB is progressively more diffuse and shallow moving from SE to NW, leading to the emersion of Pantelleria Island in the NW part of the basin (Civile et al., 2010).

The volcanic activity of Pantelleria Island started around 320 ka and the erupted units are mostly pantellerites (i.e., peralkaline rhyolites), less commonly trachytes and subordinately basalts (Civetta et al., 1984; Mahood and Hildreth, 1986). The volcanic activity has been divided into two main stages: pre- and post-Green Tuff eruption (Fig. 1b). The first stage can be further divided into two sub-phases, the first of which (between 324 and 190 ka ago) consists of effusive and explosive activity; related products are presently exposed into cliff sections, mainly along the S–SE coast of the island (unit 1 in Fig. 1b). The second sub-phase (between 190 and 46 ka ago) is characterized by several explosive (ignimbritic) eruptions, ranging in composition from trachyte to comendite/pantellerite, alternating with effusive to strombolian eruptions of pantelleritic magma from small and local centers (Jordan et al., 2018), now mostly covered by successive eruptive units. During the second sub-phase, basaltic eruptions were quite rare, with a few lava flows recognized in the NW sector of the island and dated to 118 ± 9 ka and 83 ± 6 ka (unit 2 in Fig. 1b; Civetta et al., 1984). The collapse of La Vecchia caldera (purple line in Fig. 1b) occurred during this second phase and was dated between 114 and 175 ka by different authors (Mahood and Hildreth, 1986; Rotolo et al., 2013). The second stage started with the 45.5 ± 1.0 ka-old explosive eruption of the Green Tuff (GT, hereafter) associated with the development of the Cinque Denti caldera (green line in Fig. 1b; Mahood and Hildreth, 1986; Zanchetta et al., 2018). This caldera-forming ignimbrite covers most part of the island (unit 3 in Fig. 1b), partly hindering the products of the previous eruptive history of the island. After the GT eruption, Montagna Grande dome (unit 4 in Fig. 1b) formed in the central part of the island due to

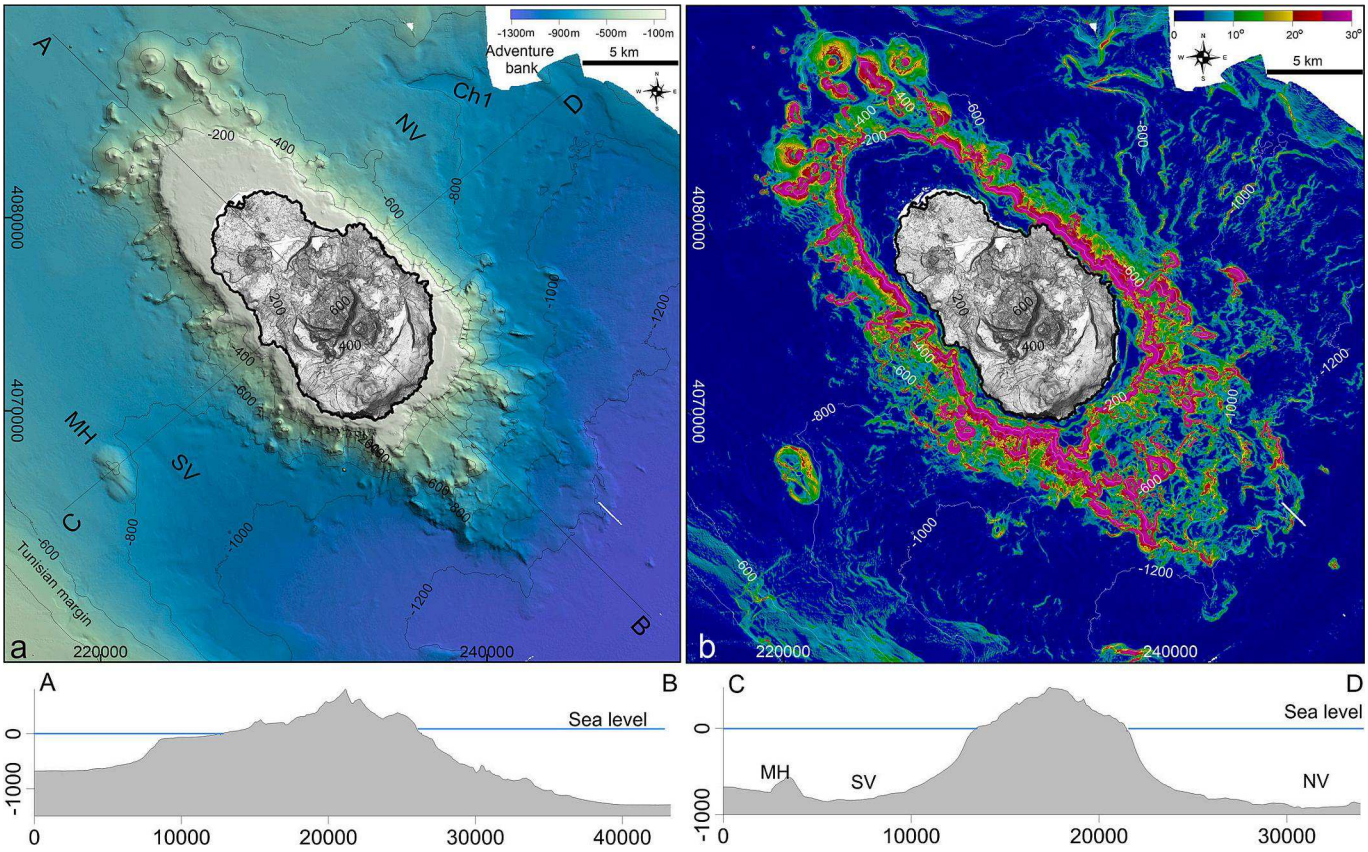

Fig. 2. Hillshade (a) and slope gradient (b) maps of the Pantelleria volcano (submarine and subaerial data from multibeam bathymetry and LiDAR aerial survey, respectively); Ch: channel; NV and SV: Northern and Southern Valleys, respectively; MH: morphological high. Below, cross-sections (location in Fig. 2a) of the Pantelleria volcano along the -SE-NW and SW-NE axis.

resurgence processes within the caldera (Orsi et al., 1991). The post-GT volcanic activity was characterized onland by the formation of several (>40) eruptive centres closely spaced in time and space and characterized by mildly explosive eruptions and/or effusive activity (Fig. 1b; Rotolo et al., 2021). Mafic eruptive centres are mostly confined to the northwest part of the island (unit 5 in Fig. 1b), with an early activity (lava flows and cinder cones) dated around 30 ka and associated with the formation of Cuddia Bruciata and Cuddia Del Monte (Fig. 1b), and a later volcanic phase occurred around 10 ka, producing Cuddie Rosse cinder cones. Felsic eruptive centres are commonly built on or near caldera faults (units 4 and 6 in Fig. 1b), forming lava shields, pumice and lava cones (Mahood and Hildreth, 1986; Civetta et al., 1988). The most recent eruption of Pantelleria was submarine and occurred in 1891 about 5 km NW of the western coast of the island (Riccò, 1892; Washington, 1909). The vent location and its morphology were identified by Calarco (2011) and Casalbore et al. (2011), while the eruptive mechanism that produces lava balloons was investigated by Conte et al. (2014) and Kelly et al. (2014).

The tectonic setting of Pantelleria Island is dominated by NE-SW and NW-SE trending extensional fault segments, kinematically compatible with a roughly E-W extension direction (Catalano et al., 2009). The distribution of eruptive fissures, dykes and eruptive centres is also aligned along the NNE–SSW belt (Fig. 1b; Civile et al., 2008), thus suggesting that crustal cracking with associated magma intrusions has occurred with a similar trend. The NNE–SSW oriented Zinedi fault is one of the most striking tectonic features (Fig. 1b), crossing the whole island and separating a NW sector, gently sloping to the sea, from the rest of the island. According to seismic evidence, the Zinedi fault continues offshore along the NE sector of the island (Civile et al., 2008). Offshore seismic data also suggest that normal faults, mainly oriented NW-SE, bound the edifice, while subordinate transverse structures are oriented E-W and NE-SW (Corti et al., 2006; Civile et al., 2008).

The oceanographic setting of the study area is characterized by three main water masses: the eastward flowing Modified Atlantic Water in the first 200 m wd; the westward-flowing Levantine Intermediate Water in the depth range 200–700 m; the westward-flowing transitional Eastern Mediterranean Deep Water at greater depths (Astraldi et al., 2001).

Regarding meteo-marine conditions, the wave regime is related to the provenance of the most energetic storms from the western Mediterranean basin. Such storms are generated by the intense NW winds (i.e., Mistral and Tramontana) and are associated with long fetches that start from the Gulf of Lion, leading to significant wave heights over 4 m (Carillo et al., 2012). Accordingly, the spatial wave energy distribution around the exposed part of the island to the NW winds is generally uniform (5.5–7 kWm^{-1}; Cavallaro et al., 2020), slightly decreasing (3–4 kWm^{-1}) along the more protected SE sector.

3. Data and methods

The submarine flanks of Pantelleria were mainly investigated during the 2006 *Zibibbo* and 2008 *Passito* cruises aboard R/V *Urania* (National Research Council). During these cruises, vessel positioning was supplied through DGPS corrections with decimetric accuracy. Bathymetric data were collected using a 50 kHz multibeam system (Reson Seabat 8160) in the depth range 20–1300 m; daily sound velocity profiles along the water column were collected using a Navitronic SVP-25 probe, while a hull-mounted sound speed sensor was used to update in real-time the sound velocity values close to the multibeam transducer for a correct beamforming. Attitude (pitch, roll, yaw and heave) data were recorded by the Inertial Navigation System Mahrs TSS; patch tests were performed at the beginning and end of each cruise.

A shallow-water (< 120 m wd) bathymetric survey around the island

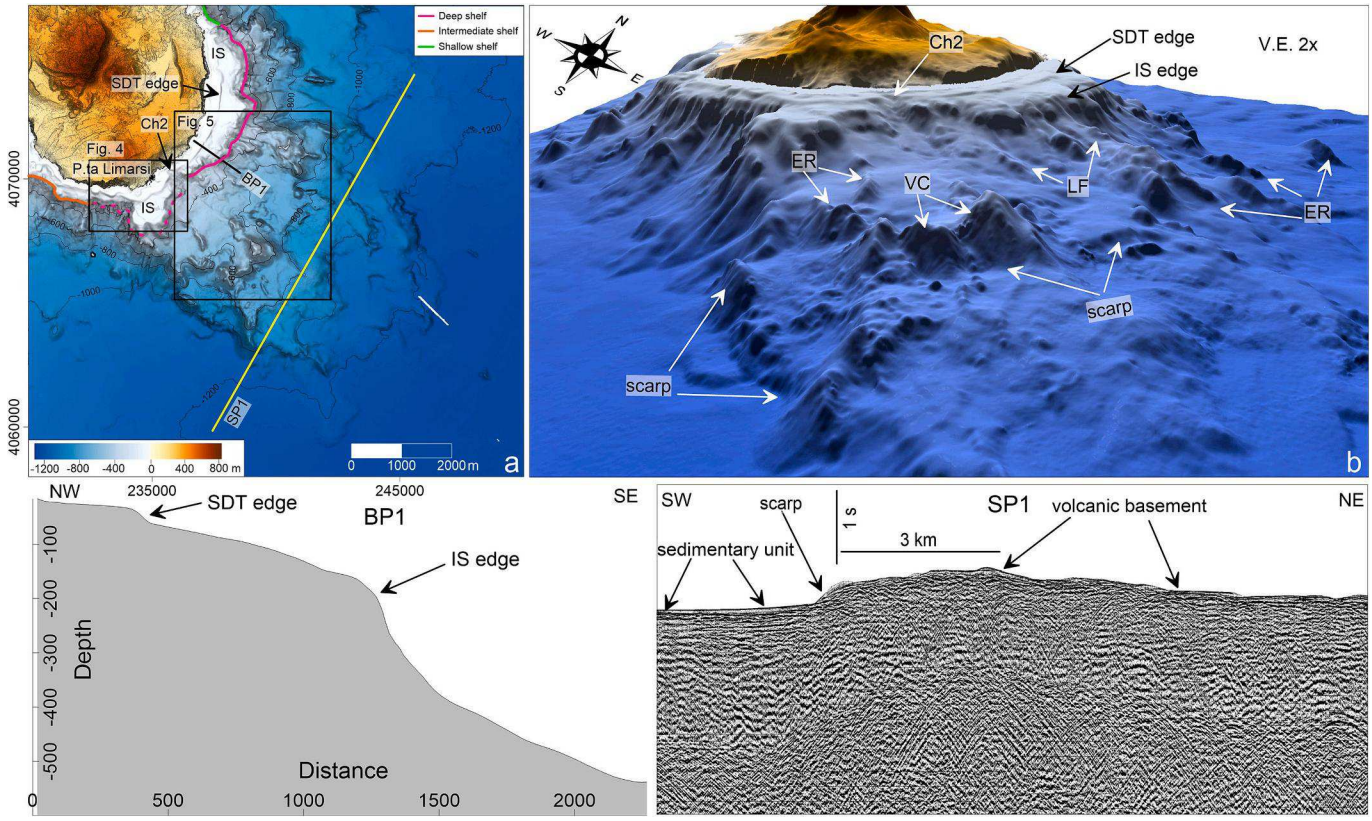

Fig. 3. Hillshade (a) and 3-D maps (b) of the south-eastern flank of the Pantelleria volcano, with the indication of the main geomorphic features and the trace of seismic (yellow line) and bathymetric (black line) profiles. IS: insular shelf; SDT: Submarine Depositional Terrace; VC: Volcanic Cone; ER: Elongated Ridge; LF: Lava Flow; V.E.: Vertical Exaggeration. Below, BP1 shows the bathymetric profile of the insular shelf and underlying volcanic flank; SP1 is a multichannel seismic reflection profile from Videpi database (https://www.videpi.com/videpi/sismica/sismica.asp), showing the different seismic facies characterizing the volcanic flank and the surrounding seafloor. (For interpretation of the references to colour in this figure legend, the reader is referred to the web version of this article.)

was performed in May 2013 using a small vessel equipped with a pole-mounted multibeam system (Reson Seabat 7125) working at a frequency of 400 kHz. Vessel positioning was supplied by an Applanix Position and Attitude System (POS/MV Wave Master) using real-time kinematic (RTK) corrections received by a temporary GNSS master base-station mounted in the island (PZIN station – RING network). In addition, raw GNSS data were recorded at both the master base station and the rover station aboard the vessel. Attitude data were recorded by Inertial Motion Unit (IMU) system at a frequency of 100 kHz for post-processing kinematic corrections (PPK) through PosPac MMS software. Final horizontal and vertical positional accuracy of this system is approximately 2 cm and 4 cm, respectively. Daily sound velocity profiles were collected using a Valeport SVP as well as real-time sound velocity close to the transducer provided by a Valeport Mini-SVS mounted on its port side.

Multibeam data collected during the different cruises were processed with Caris Hips&Sips software, where sensor data were merged and corrected for the effects of tide, roll, pitch, yaw, time delay, and sound velocity variations that occurred in the water column during survey (for further details see Bosman et al., 2015). Manual editing and automated filters were used to clean noise and spikes, and to generate Digital Elevation Models (DEMs, hereafter) with cell-sizes ranging from 0.5 m in the first 100 m wd to 10–20 m at higher depths.

The submarine DEM was integrated with that of the island (with a grid-cell size of 1 m) reconstructed from a topographical LiDAR aerial survey of Ministero dell'Ambiente e della Tutela del Territorio e del Mare.

About 640 nautical miles (n.m.) of single-channel seismic reflection data were also collected during the cruises using both the hull-mounted Datasonic Cap-6600 Chirp-II sub-bottom profiler (580 n.m.) operating at a frequency of 3.5 kHz and a towed Sparker system (54 n.m.) operating at 1.5 and 4.5 kJ with frequencies of 100–1000 Hz. In addition, high-resolution seismic data acquired using both a Chirp Swan Pro 2.02 system and a Geo-Source 1500 Sparker system were collected during the EUROFLEETS2 PANTHER (*PANTelleria High-energy ERuptions from marine studies*) cruise perfomed onboard R/V *Minerva1* (CNR) on 6–11 June 2016.

Data processing was performed through Geosuite software, while the visualization and interpretation of the seismic profiles was carried out through IHS Kingdom Suite.

Multichannel seismic profiles from the Mediterranean Sea MS lines, also called "Ministerial Seismic lines" were also examined using the VIDEPI website (https://www.videpi.com/videpi/videpi.asp).

4. General morphology of the Pantelleria edifice and surrounding areas

The acquired morpho-bathymetric data show that Pantelleria island is the upper part (~18%) of a large submarine volcanic edifice, ~36 km long and ~ 15 km wide, encompassing a surface of approximately 310 km^2 (Fig. 2). The volcanic edifice is markedly elongated along a NW-SE direction and rises from the Pantelleria Basin (PB in Fig. 1a), whose floor becomes shallower moving towards the NW. Following this bathymetric trend, the base of the Pantelleria edifice can be morphologically traced down to 1300 m wd on the SE flank, 700/900 m wd on NE and SW flanks, and <700 m on its NW flank (Fig. 2a and related bathymetric profiles). The Pantelleria volcano divides the northern part of the Pantelleria Basin in two valleys (Calarco, 2011):

-the northern valley (NV in Fig. 2a) is approximately 8 km wide and bounded to the north by the Adventure Bank slope, on the south-western Sicilian margin; its floor is characterized by an uneven morphology

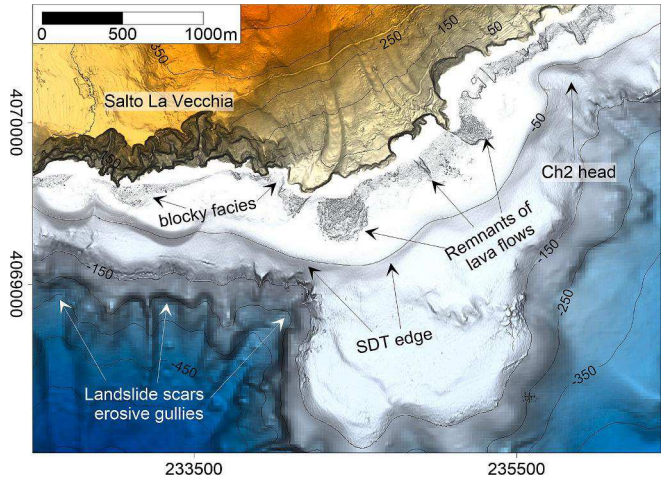

Fig. 4. Zoom of the SE insular shelf (location in Fig. 3), showing the presence of a blocky facies and remnants of lava flows in the nearshore sector passing downslope to a smooth seafloor associated with the formation of a submarine depositional terrace (SDT). The insular shelf and SDT edge are also affected by mass-wasting processes.

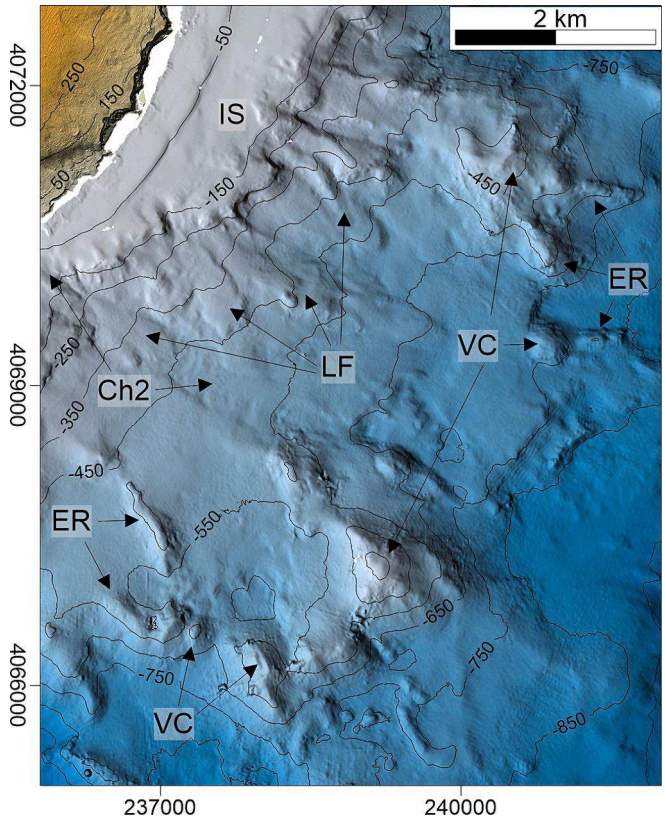

Fig. 5. Zoom of the south-eastern flank of Pantelleria (location in Fig. 3), better evidencing the occurrence of lava flows (LF) in upper slope, while partially dismantled volcanic cones (VC) and elongated ridges (ER) are recognizable downslope.

(Fig. 2a and b; see also section 4.3);

-the southern valley (SV in Fig. 2a) is approximately 5 km wide and bounded by the lower slope of the Tunisian continental margin. The SV floor shows a more subdued morphology with respect to the NV, except for an NNW-SSE elongated morphological high (MH in Fig. 2a and profile C—D), approximately 200 m high, 3 km long and 1.6 km wide (for details refer to Martorelli et al., 2011).

The volcanic flanks of the Pantelleria edifice are characterized by different slope gradient (Fig. 2b), as well as by a large variability in primary (volcanic) and erosive-depositional geomorphic features, as described below. Based on main morphological characteristics the volcanic edifice can be divided in four main sectors, hereafter described: the SE, SW, NE, NW submarine flanks.

4.1. The submarine SE flank

The SE flank is the deepest submarine sector of Pantelleria, showing a very complex morphology (Figs. 2 and 3). In the shallower portion, it is characterized by a 1–2 km wide insular shelf (IS in Fig. 3a), with the edge located between 100 and 210 m wd, except off P.ta Limarsi where the shelf is markedly narrower and shallower due to the occurrence of a shelf-indenting channel (Ch2 in Figs. 3 and 4). In detail, most part of the shelf edge lies at water depths >200 m (magenta line in Fig. 3a, section BP1), shallowing at 140–160 m wd in the SW part (orange line in Fig. 3a) and around 100 m wd in the NE-most part (green line in Fig. 3a). The shelf has average slope gradients of 2°-6° in the first 100 m wd, increasing up to 15–20° down to 210 m (Fig. 2b). The shelf surface shows an overall smooth morphology, with the presence of a main submarine depositional terrace (SDT in Figs. 3 and 4, profile BP1) with edge at water depths between 30 and 50 m, running roughly parallel to the coastline (Fig. 3b). Only in the first 15–35 m of depth, a blocky facies with remnants of lava flows are recognizable (Fig. 4).

Below the IS edge, slope gradients markedly increase to values higher than 30° (locally reaching 60°, section BP1 in Fig. 3) and then gradually decline to a few degrees at 1200 m wd (Fig. 2b). Several volcanic features are recognizable along this submarine flank, including: i) a few kilometers-long and some hundred meters-wide along-slope features interpreted as lava flows (LF in Fig. 3b and 5), mostly located in the upper slope down to 500–600 m wd; ii) the remnants of radially elongated ridges (ER in Fig. 3b and 5) oriented along the SE-NW (mostly), NE-SW and NNW-SSE directions; iii) clusters of partially eroded volcanic cones (VC in Fig. 3b and 5), with diameters variable from few hundreds of meters up to 1 km, and elevated tens of meters above the surrounding seafloor. They are often delimited by steep escarpments, up to 200-m high, mainly oriented along NW-SE and SW-NE directions (Figs. 2b and 3b). Erosive features are widespread, including landslide scars with diameter of few hundred meters, gullies and channels that carve both the previously described volcanic features as well as the edge of the IS and SDT (Fig. 4). One of the main erosive features is the above-mentioned channel Ch2, whose head cuts back up to 35 m wd, a few hundreds of meters from the coast. On the multichannel seismic reflection profile (SP1 in Fig. 3) located between 800 m and 1000 m wd, a chaotic and hyperbolic seismic facies associated with a volcanic basement characterizes the lower SE submarine flank of Pantelleria, whereas a more stratified seismic facies associated with a sedimentary unit is recognizable in the southern area (SV in Fig. 2). High-resolution Chirp profile (Fig. 1 ESM), crossing the Southern Valley, shows a 5–10 ms thick, acoustically semi-transparent unit above a high-amplitude reflector characterized by a regular geometry.

4.2. The SW flank

The SW flank is steeper and narrower than the SE flank (Fig. 2, profile C—D). In this sector, the IS is relatively narrow (600–900 m wide), with the edge located between 100 and 160 m wd, except off Scauri and Cala di Sataria, where it is almost absent due to two shelf-indenting channels (Ch3 and Ch4 in Fig. 6). In detail, the shelf edge located to the south of Scauri (orange line in Fig. 6a) lies at depths of 145–160 m, while it is generally shallower than 130 m northward of Scauri (green line in Fig. 6a). The shelf morphology is characterized by a blocky facies in the near-shore sector, passing downslope to a smoother seafloor, except off P.ta Ferreri where a partially-eroded and 500 m wide

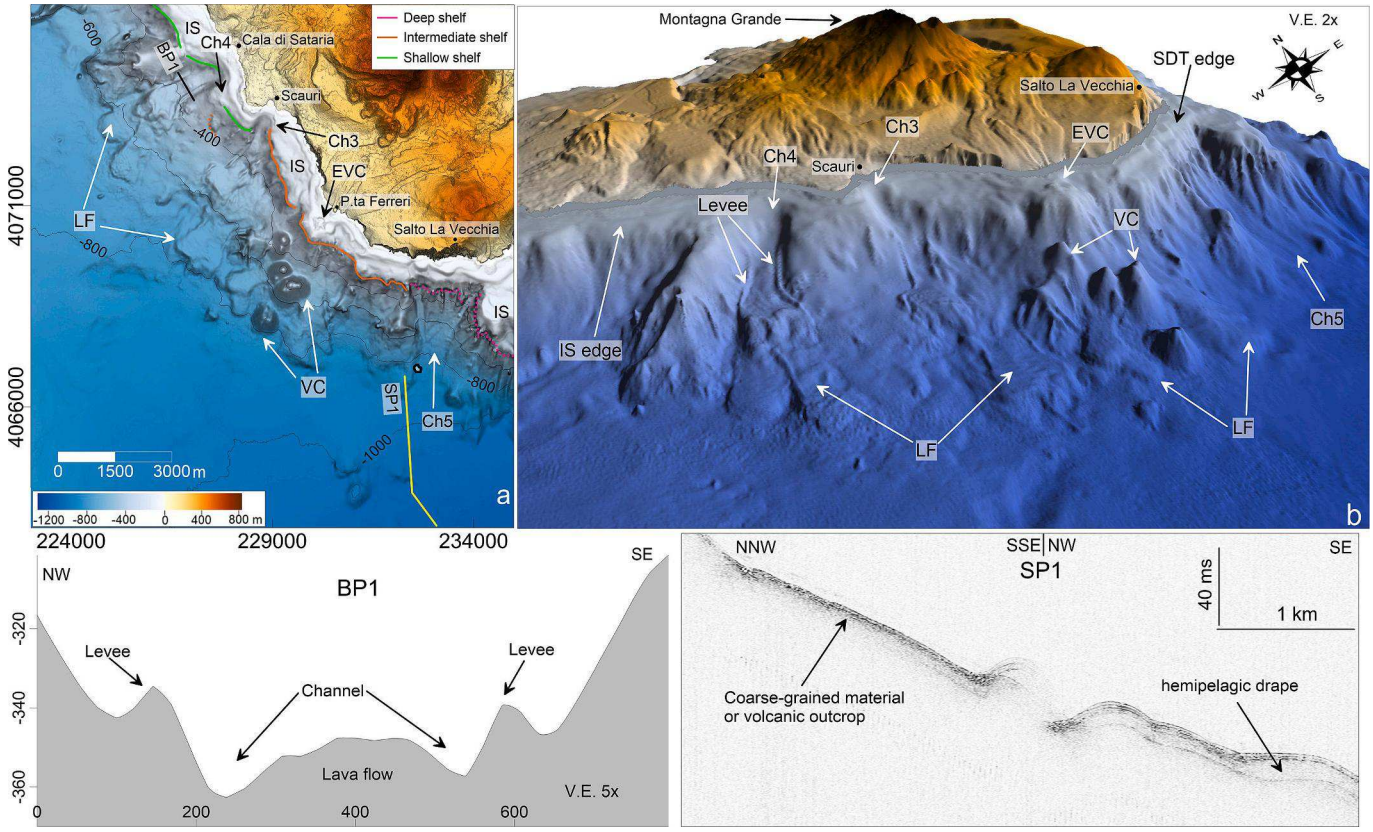

Fig. 6. Hillshade (a) and 3-D maps (b) of the south-western flank of the Pantelleria volcano, with the indication of the main geomorphic features and the trace of seismic (yellow line) and bathymetric (black line) profiles. Acronyms as in the previous figures; EVC: Eroded Volcanic Centre on the shelf. Below, section BP1 shows the channel-levee morphology that characterizes the upper part of the large lava flows here present; Chirp profile SP1 shows the different seismic facies recognizable between the lower flank of Pantelleria volcano and the surrounding seafloor. (For interpretation of the references to colour in this figure legend, the reader is referred to the web version of this article.)

cone-shaped feature (EVC in Fig. 6) is present. The smooth seafloor is due to the occurrence of two SDTs, with the edge located at depths of 30–45 m and 60–70 m wd, respectively (Fig. 6).

Below the IS edge, the slope gradients increase to values higher than 30° and then rapidly decrease to a few degrees at the base of the edifice (Fig. 2b). This submarine flank is dominated by different morphological features related to past volcanic activity, including a series of stacked, multidirectional and thick features interpreted as lava flows off Scauri village (LF in Fig. 6). These lava flows are approximately 1 km-wide and few kms-long; they are characterized by roughly linear channel-levee morphology in their upper part, i.e., from 300 down to 600 m wd. Levees are up to 20 m high (BP1 in Fig. 6) and lie on slope gradients of about 16°. The best preserved volcanic morphologies are a cluster of four volcanic cones (VC in Figs. 6 a and b) observed off P.ta Ferreri. These cones have basal diameters of 500–800 m and height of 120–210 m with respect to the surrounding seafloor and some of them show the presence of lava lobes at their base and around (LF in Fig. 6b). In this sector, erosive features are widespread, with small landslide scars affecting the edge of the IS and representing the headwall of steep gullies that merge downslope in larger and flat-bottomed channels, as for instance observed off Salto La Vecchia (Ch5 in Fig. 6). Chirp profile (SP1 in Fig. 6) shows high-amplitude reflections and lack of penetration along the lower volcanic flank and channel floor where coarse-grained material or volcanic outcrop is present, while at greater depths an acoustically semi-transparent unit is present, characterized by superficial high-amplitude reflections, suggesting a hemipelagic drape with an average thickness of 10 ms (T.W.T.).

4.3. The NE flank

The NE flank is also relatively narrow and steep (Fig. 2, profile C—D). It is characterized by a narrow (400 m) or almost absent insular shelf (such as off Khaggiar lava flows, where lava flows reached the coast and prograded on the shelf, Fig. 7a and BP2) in the southern part, enlarging up to 1 km only in the northern part. The shelf edge is commonly located at water depths <110 m (green line in Fig. 5a).

In the southern part, the shelf is mostly characterized by a blocky facies alternated with lava flows (Fig. 8), while an overall smooth morphology is recognizable where the shelf widens in the northern sector (Fig. 7a). Here, two orders of SDT are recognizable, with the edge located at water depths of 30–45 m (the main one and most continuous) and 60–70 m, respectively. A seismic profile crossing the shallower SDT (SP1 in Fig. 7) shows the occurrence of a stratified unit made up by a succession of high to medium-low amplitude reflections with good continuity. This unit has a maximum thickness of 20 ms (T.W.T) and rests above a high amplitude irregular reflection, representing the top of the acoustic basement. The stratified unit can be divided into two sub-units: the lower one is characterized by sub-parallel, medium to low amplitude and continuous reflections; the upper one is made up by oblique-sigmoidal, medium to low amplitude reflections, downlapping on the lower unit.

The remnants of a volcanic cone (EVC in Fig. 7a, see also cross-section BP1), with average diameter of few hundreds of meters, height of few tens of meters with respect to the surrounding seafloor, and summit at ~15 m wd, are recognizable on the shelf off the northern segment of the Zinedi Fault.

Below the shelf edge, slope gradients markedly increase to values

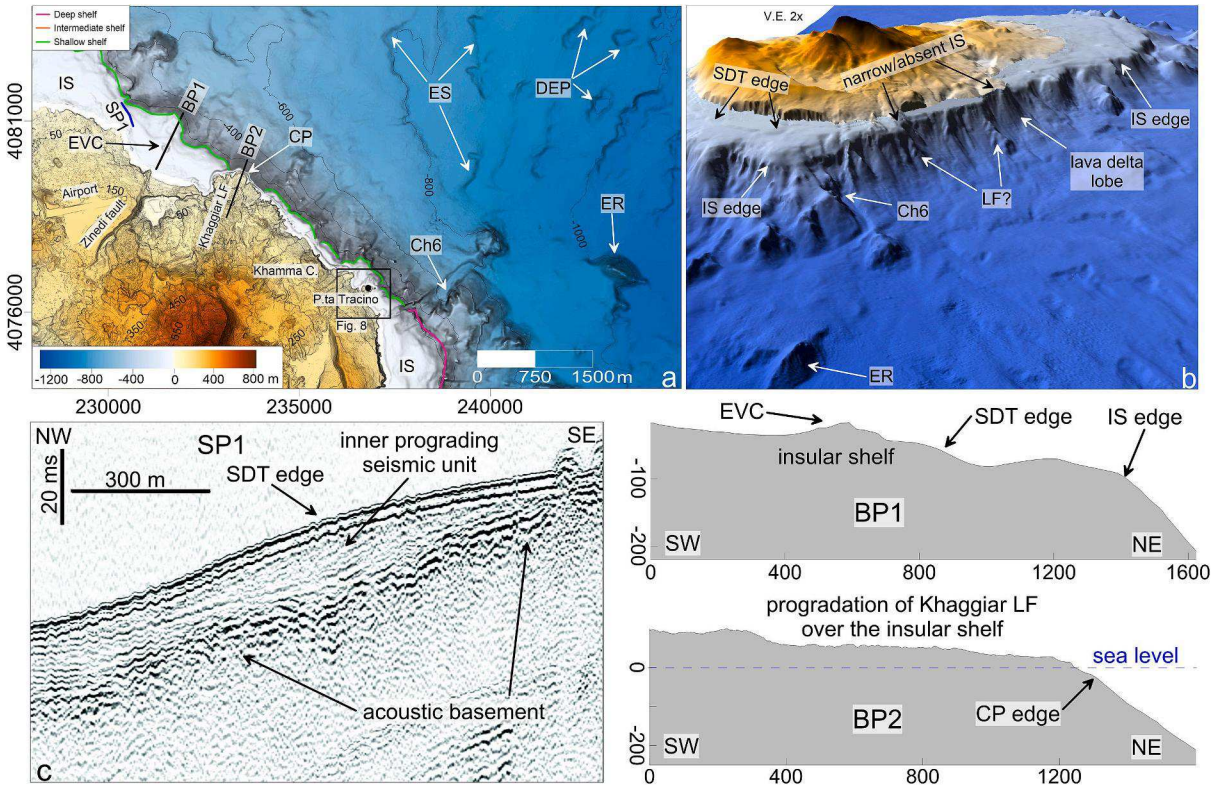

Fig. 7. Hillshade (a) and 3-D maps (b) of the north-eastern flank of the Pantelleria volcano, with the indication of the main geomorphic features and the trace of seismic (blue line) and bathymetric (black line) profiles. Acronyms as in the previous figures; DEP: enclosed depression; ES: erosive scarps. The Sparker SP1 profile, crossing the submarine depositional terrace (SDT), shows its inner prograding geometry that overlies the acoustic basement. Section BP2 shows the progradation of the Khaggiar lava flows (LF) over the insular shelf, forming a coastal platform(CP) with edge around 15–25 m wd, while the original insular shelf is preserved just to the north, with edge around 110 m wd (section BP1). (For interpretation of the references to colour in this figure legend, the reader is referred to the web version of this article.)

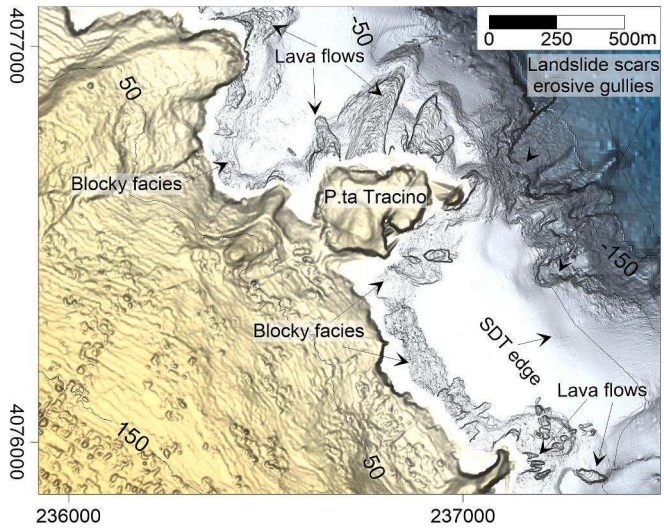

Fig. 8. Zoom of the insular shelf off Punta Tracino (location in Fig. 7), showing the presence of a blocky facies and lava flows in the nearshore sector. Note the smooth seafloor downslope associated with the formation of a submarine depositional terrace and mass-wasting processes affecting the insular shelf edge.

higher than 30° and then markedly decrease downslope (Fig. 2b). This flank is characterized by along-slope volcanic features that often appear in morphological continuity with the main volcanic structures observed onland (Fig. 7b). Erosive-depositional features are recognizable along this flank, mostly represented by small (few hundreds of meters wide) landslide scars affecting the IS or SDT edge in the depth range 40–100 m water depth, and by gullies (Figs. 7 and 8). A main channel (Ch6 in Fig. 7a) is located south of P.ta Tracino; its headwall is made up by two branches that cut back to 30 m water depth, a few hundreds of meter from the coast (Fig. 7b). An uneven morphology is present in the North Valley (NV in Fig. 2), bounding the NE flank of Pantelleria, due to the occurrence of different erosive-depositional features, such as erosive scars, coaxial trains of crescent-shaped bedforms and enclosed depressions (ES, CSB and DEP in Fig. 9a). On Chirp profiles, the NV is generally characterized by an acoustically semi-transparent seismic units associated with hemipelagic drape, overlying a high amplitude reflection with irregular geometry (Figs. 9 b and c). On Sparker profile (Fig. 8d), this high-amplitude reflection corresponds to the top of a stratified seismic unit. It is noteworthy that in the Southern Valley, the acoustically semi-transparent unit overlies a high-amplitude reflector but characterized by a regular geometry.

4.4. The NW flank

The NW flank is wide and generally gently sloping (Fig. 2, profile A—B), being characterized by a 4 km-wide shelf in the semi-circular sector encompassed between P.ta Fram and P.ta Karuscia; the shelf becomes narrower (500–800 m) towards the SW and NE sectors (Fig. 10a). Accordingly, the shelf edge is generally located at about 120–130 m wd in the widest shelf sector (green line in Fig. 10a), except for a small part lying at depths around 150–160 m (orange line in Fig. 10a) and becoming shallower (around 100 m wd) towards the NE and SE sectors. The shelf has a very rugged morphology due to the presence of a blocky facies alternated with lava flows down to 50 m wd, where the remnants

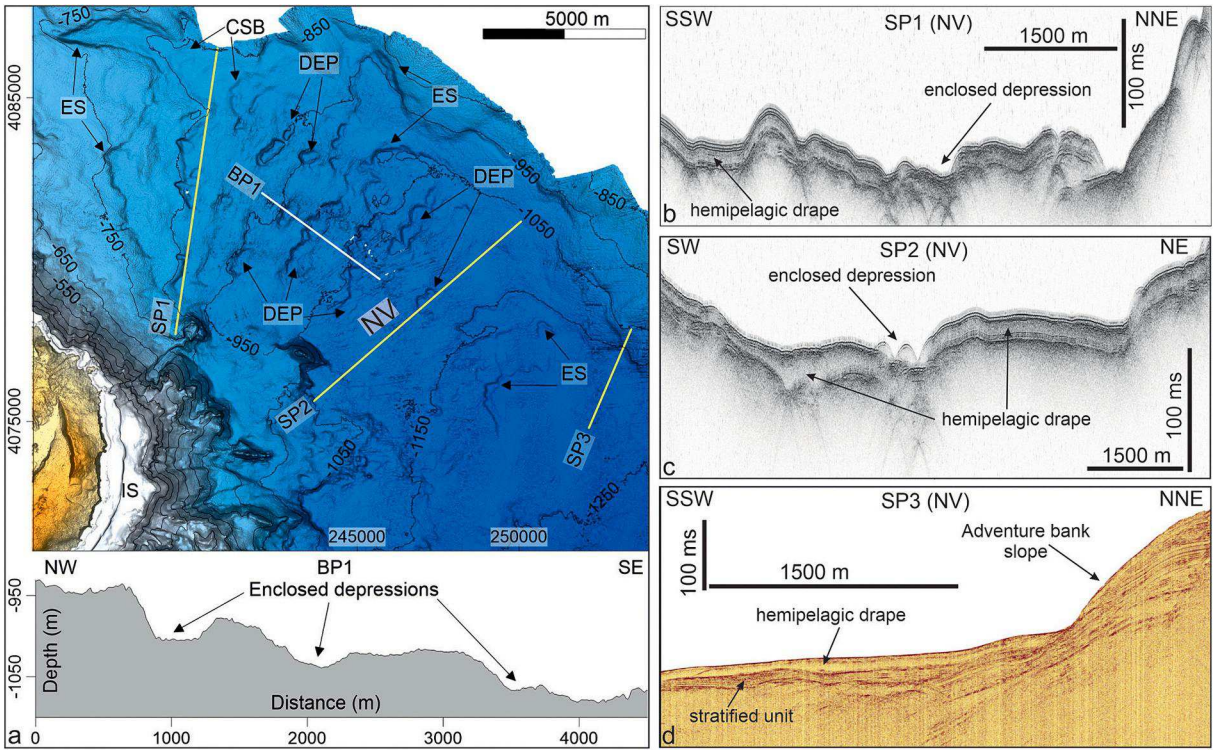

Fig. 9. a) Zoom of the North Valley, characterized by an uneven morphology due to the presence of erosive scars (ES), crescent-shaped bedforms (CSB) and enclosed depressions (DEP), as evidenced by section BP1. SP1 (b) and SP2 (c) Chirp profiles showing the presence of an acoustically semi-transparent unit, bounded at its base by high amplitude and irregular reflection. This unit has been interpreted as hemipelagic drape and shows lateral variation in thickness. d) SP3 Sparker Profile showing the presence of the hemipelagic drape (semi-transparent seismic unit) above a stratified unit. Note that the hemipelagic drape is characterized by lateral variations in thickness and shows an external mounded shape at the foot of the Adventure bank slope, which can be interpreted as a small contourite drift.

of two small and sub-circular volcanic centers are still recognizable (EVC in Fig. 10). At greater depths, the shelf has a smoother morphology with an average slope of 2°, being locally interrupted by a series of morphological steps (MS in Fig. 10), located at water depths around 66, 78 and 114 m. In plan-view, these slope breaks have irregular shape, suggesting a morphological control from subdued features.

Below the shelf edge, the flanks are markedly steeper (20°-30° in the upper part, rapidly decreasing to a few degrees at water depths >600 m; Fig. 2b), except for a small sector in the NW-most part of the shelf, where the IS edge is deeper (orange line in Fig. 10a), This edge lies on a 1-km wide ridge, which is characterized by a smooth and relatively gently sloping (on average 7°) summit down to 210 m wd, becoming steeper (up to 14°) downslope (Fig. 10). Most part of the NW flank is characterized by a large (85 km^2) field of volcanic cones (VC in Fig. 10), which represents one of the most striking volcanic features of the Pantelleria offshore. The volcanic field is formed by 26 well-preserved volcanic cones (including the one associated with the 1891 eruption, see Conte et al., 2014), with basal diameters ranging between 200 and 3500 m and heights of 40–345 m with respect to the surrounding seafloor. The base of the volcanic cones is located between ~300 and ~ 700 m wd, while their summit lies between 614 and 165 m wd. The volcanic cones have conical to elongated shape in plan-view, even if composite features, created by coalescent vents, are recognizable. Most volcanic cones display a preferential morphological orientation (mainly along the SE-NW direction and secondarily along the SW-NE direction), often resulting from the alignment of single conical vents along narrow eruptive fissure ridges at their summit (EF in Fig. 10). The volcanic cones are mostly pointy and generally characterized by steep (20°-40°) and smooth flanks. A few volcanic cones show horseshoe-shaped summit and lateral collapse (Fig. 10b). Within the upper part of the cones, the occurrence of resurging, well-preserved vent is locally observed (section BP1 in Fig. 10). Erosive-depositional features along this flank include small (few hundreds of meters in diameter) landslide scars locally affecting the insular shelf, two main channels and a landslide deposit. The first channel (Ch7 in Fig. 10a) is ~1 km-wide and ~ 2 km-long, affecting the NW edge of the shelf. The second channel (Ch8 in Fig. 10a) is located in the south-western part of the volcanic field; it is 3.5 km long and 150–600 m wide. The channel thalweg is floored by crescent-shaped bedforms (BF in Fig. 10 and related bathymetric section BP2), with wavelength of 200–320 m and wave height of 2–6 m, progressively increasing in wavelength and lateral extent downslope. A lobate deposit with a morphological relief of 10–15 m with respect to the surrounding seafloor and rough superficial morphology, is recognizable in this area; it has been interpreted as a (partially covered) blocky landslide deposit (LD in Fig. 10 and related bathymetric section BP3). Multichannel seismic profile crossing the lower volcanic flank (Fig. 11a) shows a chaotic and hyperbolic seismic facies characterizing the volcanic field with respect to the more stratified seismic facies associated with the sedimentary unit of surrounding areas. Moreover, this stratified facies is also present within the topographic lows located between the main volcanic cones, representing a sedimentary infilling. High-resolution seismic profiles (Sparker in Fig. 11b and Chirp in Fig. 11c) show the different thickness of the stratified seismic facies between the volcanic cones and the surrounding seafloor. This stratified unit is overlain by an acoustically transparent facies that can be interpreted as hemipelagic drape.

5. Discussion

The morpho-bathymetric analysis of the submarine part of Pantelleria volcano, integrated by selected seismic reflection profiles, allowed us to map the main features characterizing its flanks and to discuss the interplay between volcanic, tectonic, and erosive-depositional processes in shaping the volcano, also through

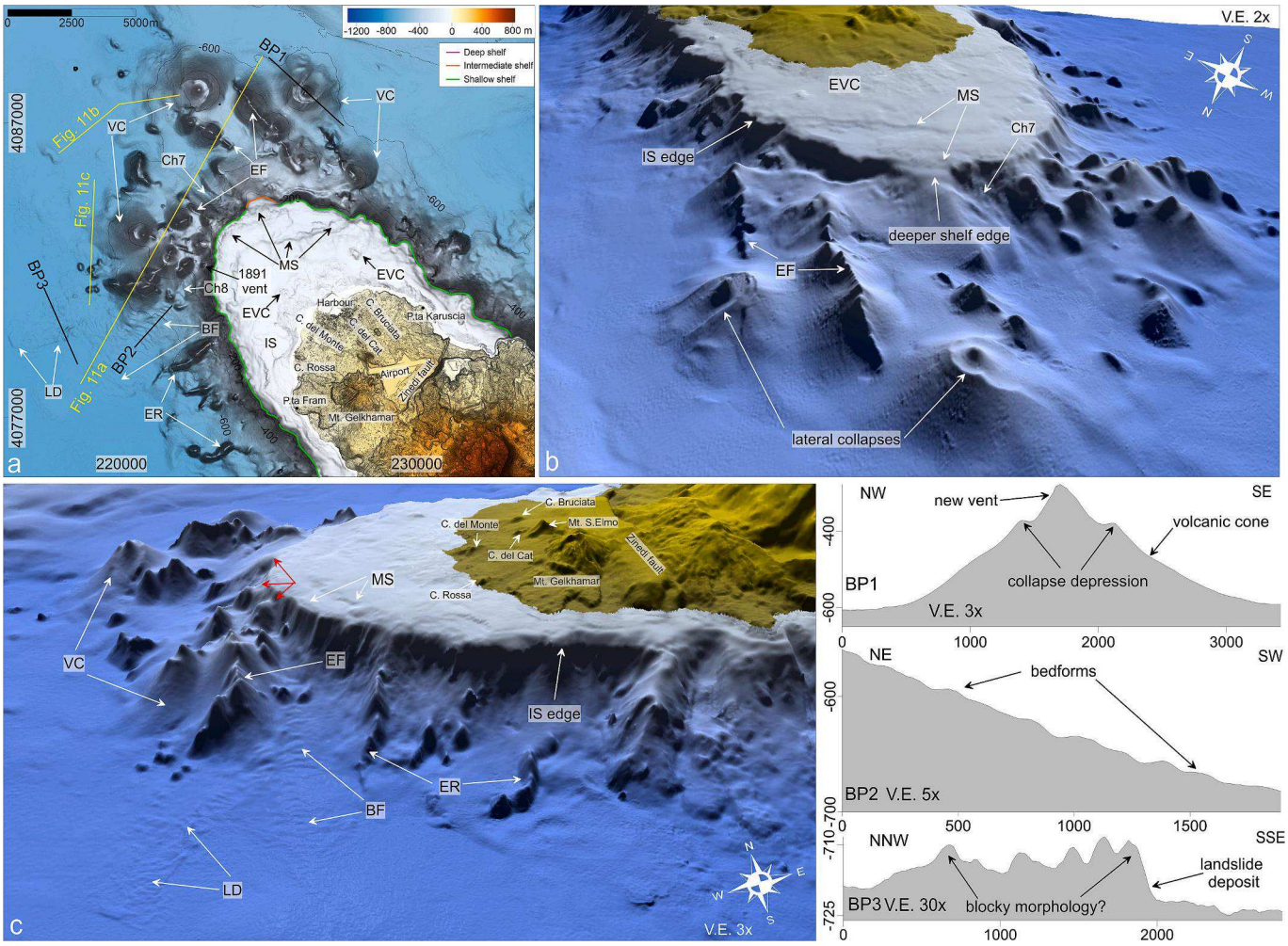

Fig. 10. Hillshade (a) and 3-D maps (b and c) of the north-western flank of the Pantelleria volcano, with the indication of the main geomorphic features and the trace of the bathymetric (black line) and seismic (yellow line) profiles shown in Fig. 11. Red arrows indicate volcanic cones characterized by a truncation in correspondence of the insular shelf. Acronyms as in the previous figures; MS: Morphological Step; EF: Eruptive Fissure; BF; bedform field; LD: landslide deposit. On the lower-right, bathymetric sections showing the collapsed cones (BP1), the train of coaxial bedforms (BP2) and the blocky landslide deposit (BP3). (For interpretation of the references to colour in this figure legend, the reader is referred to the web version of this article.)

morphological comparison with other insular volcanoes (section 5.1). Furthermore, observations from the large submarine portions of the volcanic edifice give hints on its overall spatial and temporal evolution, also providing new insights on the vertical movements that affected the different sectors of the edifice during the Late-Quaternary (section 5.2).

5.1. *The interplay of volcanic, tectonic, and erosive-depositional processes in shaping the submarine flanks of Pantelleria*

The Pantelleria volcano is characterized by a predominance of primary volcanic morphologies with respect to erosive-depositional features (Fig. 12). This setting also characterizes other insular volcanoes lying in rift setting, such as the nearby Linosa (Romagnoli et al., 2020), Terceira (Azores, Casalbore et al., 2015) or submarine volcanoes in the Okinawa Trough and Amami rift (Minami et al., 2022 and reference therein). This is very different from what typically observed in volcanoes lying in arc-setting, where erosive-depositional processes largely overwhelm primary volcanic features (e.g., Carey, 2000), as, for instance, observed in the Aeolian Arc, where >70% of the seafloor is affected by mass-wasting (Chiocci and Casalbore, 2017).

5.1.1. *Interaction between tectonics and volcanism*

The Pantelleria volcano lies in a NW-SE rift zone and is strongly asymmetric, especially considering the whole subaerial and submarine structure (i.e., NW-SE length is almost 3 times higher than the NE-SW one, Fig. 2). Accordingly, the NE and SW submarine flanks of the volcano are straight and steep (Fig. 2a and b), possibly fault-controlled (Civile et al., 2008). Besides this first-order structural control in the overall development of the Pantelleria volcano, the interaction between volcanism and tectonics is clearly evidenced by the preferential elongation and/or alignment of volcanic cones and ridges along the (main) SE-NW and (secondary) SW-NE directions, in agreement with the main regional tectonic features observed on the island, in the PB and, more generally, in the Sicily Channel (Civile et al., 2008 and 2010). The development of aligned or elongated cones can be related to: a) eruptions along linear vents, as recognized in subaerial fissure swarms (e.g., Gudmundsson, 1986; Smith and Cann, 1993), b) linear chains of pointy cones along a magma-feeding fissure, creating elongated or complex structures (e.g., Corazzato and Tibaldi, 2006), and c) central volcanism focused on a single eruptive fracture (Briais et al., 2000), with the formation of isolated cones (Head et al., 1996). These processes may be also witnessed, in the NW flank of Pantelleria, by the occurrence of narrow and steep-sided ridges (EF in Fig. 10) present at the summit of isolated or coalescing volcanic cones, interpreted as the result of fissure eruption. The orientation of these features should reflect the direction of the principal stress axes during their emplacement (e.g., Fialko and Rubin,

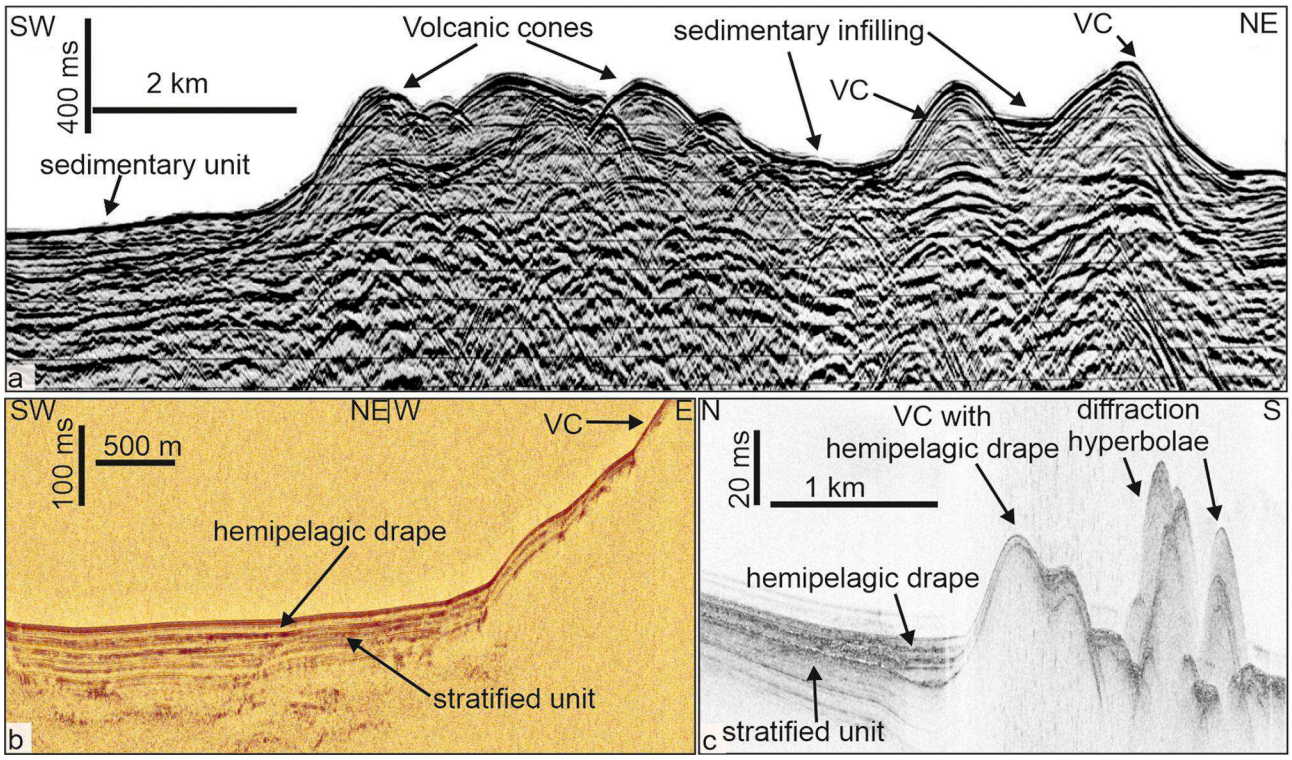

Fig. 11. a) multichannel seismic reflection profile from Videpi database (https://www.videpi.com/videpi/sismica/sismica.asp), showing different seismic facies of volcanic cones and surrounding seafloor; also note the presence of sedimentary infilling in bathymetric lows among the volcanic cones. b) Sparker profile showing the variable sedimentary cover from the flank of a volcanic cone to the surrounding seafloor. c) Chirp profile showing the variable thickness of hemipelagic drape among the volcanic cones and surrounding seafloor. Location of the seismic profiles in Fig. 10a.

1999). In the SE submarine flank of Pantelleria, the volcano-tectonic interaction is also evident, because erosional processes (see further on in discussion) enhanced the morphology of volcanic structures according to their erodibility. Here, several elongated ridges are present (ER in Fig. 3) along with steep and hundreds meters-high scarps, mainly oriented along NW-SE and SW-NE directions. These scarps are likely tectonically-controlled, as previously inferred through seismic profiles by Civile et al. (2008).

Despite the marked asymmetry in the distribution of volcanic and tectonic features and the locally high slope of its submarine flanks, surprisingly no large-scale flank collapse is observed along the flanks of the Pantelleria volcanic edifice, while its volcano-tectonic evolution was characterized by multiple caldera collapses in the subaerial part. Different factors can be addressed to explain this setting, such as the lack of a main volcanic axial zone at Pantelleria volcano (as for instance observed at Stromboli Island; Romagnoli et al., 2009) or its maximum height (2100 m) less than the critical value of 2500 m identified through a susceptibility analysis to large-scale landsliding performed on oceanic volcanic islands and seamounts (Mitchell, 2003). However, we are aware that further data would be required for better constrain the role of these factors (or additional ones) in controlling the formation of such catastrophic collapses, but this issue is beyond the aim of this paper.

5.1.2. *Volcanic features*

Regarding the spatial distribution of primary volcanic features on the submarine flanks, volcanic cones and elongated ridges dominate the offshore sectors (Fig. 12), while lava flows are observed both in shallow-water (Figs. 4, 8, 10) and deep-water (Figs. 5 and 6) areas. In the mostly constructional, NW flank of Pantelleria, a cluster of 26 well-preserved volcanic cones are recognized, showing smooth and steep flanks similar to that of monogenetic scoria cones formed by the eruption of low-viscosity magma on strombolian, hawaiian or phreatomagmatic eruptions (Sigurdsson et al., 2000; Fornaciai et al., 2012). These findings agree with the observation and petrochemical analysis of the 1891 erupted products performed by Conte et al. (2014), showing an overall alkali-basalt composition, similar to the Pantelleria subaerial less-evolved products, largely outcropping in the NW sector of the island (Civetta et al., 1988; White et al., 2009; Giuffrida et al., 2020). The age of this volcanic field is unconstrained (except for the last activity of the small cone associated with the 1891 eruption). However, the morphological differences between the cones (Fig. 10) let us to hypothesize multiple stages of volcanic activity. A few cones are also affected by small-scale lateral collapses, with the re-growth of a smaller vent inside the scar collapse (Fig. 10b), indicating that the evolution of such cones can be more complex than expected, and testifying the pulsating nature of submarine volcanism. This is clearly evidenced by bathymetric and hydroacoustic monitoring both of the Monowai volcano in the Kermadec arc (e.g., Wright et al., 2008; Watts et al., 2012) and Tagoro volcano in the Canary Archipelago (Somoza et al., 2017), where similar processes have repeatedly occurred in a time span of years. Another small cluster of volcanic cones with smooth flanks is present in the SW sector of Pantelleria (just off P.ta Ferreri, Fig. 6b), indicating a similar eruptive mechanism, despite their composition could be related to more evolved magma source (Calarco, 2011).

Lava flows are mainly observed on the insular shelf, especially along the NW and NE flanks (Figs. 4, 8 and 10). They can be related to effusive activity that characterized the post-GT (< ~45 ka) evolution of Pantelleria island, with the predominance of basaltic lava flows along the NW coast and pantellerite lava flows along the NE sector (Rotolo et al., 2021 and reference therein). The latter ones are typically characterized by a well-defined shape and rough textures, as evidenced at P.ta Tracino by Abelli et al. (2016) (Fig. 8). One of the few examples of well-preserved lava flows extending even beyond the shelf edge is recognizable in the SW sector of Pantelleria offshore Cala di Sataria (Fig. 6a). Here, lava flows are likely characterized by a felsic composition, considering the petrochemical characteristics of the volcanic rocks

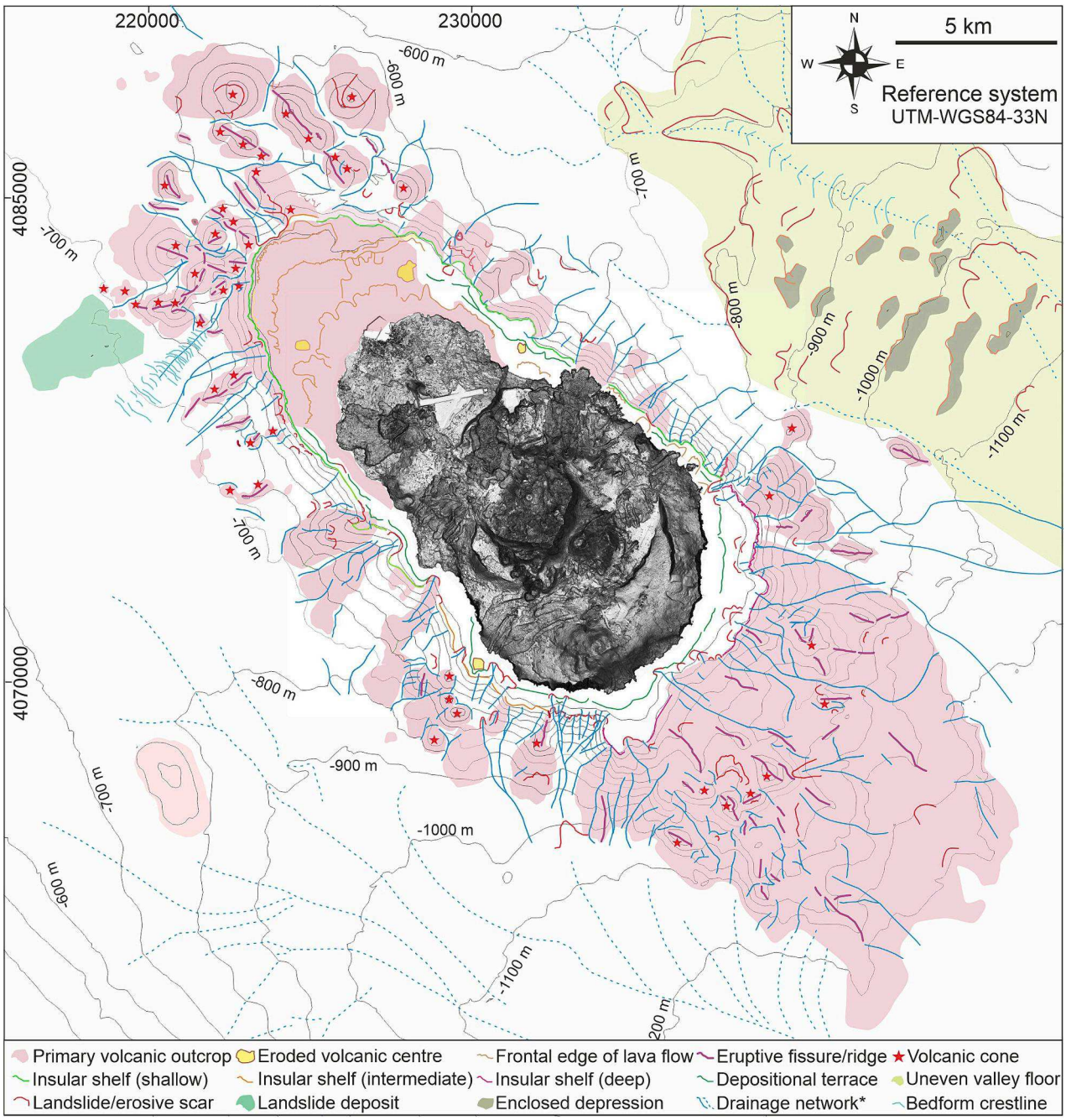

Fig. 12. Interpretative geomorphological map of the Pantelleria volcano and surrounding areas, with the indication of the main primary volcanic and erosive-depositional features. Volcanic cones and eruptive fissures/ridges dominate the morphology of the Pantelleria flanks; their elongated shape or alignment indicates a strong interaction between volcanic and tectonic processes mainly along the SE-NW and secondarily SW-NE directions. Remnants of lava flows are mainly confined to the insular shelf, especially along the NW and NE sectors (see also Figs, 4 and 8); at greater depths, lava flows are recognizable on the SW and SE flanks (Figs.5 and 6). Erosive-depositional features are divided into two main types: features related to wave reworking during Late-Quaternary sea-level fluctuations, such as the insular shelf and submarine depositional terrace, and features related to mass-wasting processes. The latter ones include landslide scars and downslope gullies/channels (solid light-blue lines) forming the drainage network of the volcanic edifice. The drainage network of the main valleys bounding the volcanic edifice is indicated by dashed blue lines. Note the widespread occurrence of erosive-depositional feature on the Northern Valley, creating an uneven seafloor morphology (see also Fig. 9). (For interpretation of the references to colour in this figure legend, the reader is referred to the web version of this article.)

outcropping on the facing subaerial sector, and the felsic composition of a rock sample recovered by one of these lava flows through dredging (Calarco, 2011). This hypothesis is consistent with their well-preserved morphologies, similar to what observed for other felsic lava flows elsewhere, such as the multiple lava flows emitted at Le Havre caldera at 1000–1500 m wd during the 2012 eruption (Ikegami et al., 2018) or the Rocche Rosse obsidian-rich rhyolite coulèe emplaced along the subaerial and submarine flank of Lipari down to 700 m wd in historical time (Casalbore et al., 2016 and reference therein). The submarine lava flows in the SW flank of Pantelleria shows a channel-levee morphology (Fig. 6b and section BP1), similarly to what commonly observed in subaerial lava flows (e., Harris et al., 2004) but being not so common for submarine lavas, where this kind of morphology has been associated with very high eruptive rate and volumes (Gregg and Smith, 2003). Moreover, the formation of well-developed levees might be related to the confinement effect exerted by the narrow channel where the lava

flowed that, in turn, is likely influenced by the steep gradients of the Pantelleria volcanic flank, similar to what shown by laboratory investigations (Gregg and Fink, 1995 and 2000). This behaviour has been observed in several subaerial Hawaiian lava flows, where higher levees are often associated with narrow and long-lived channels (e.g., Dietterich and Cashman, 2014), while flow thickness is reduced when lava flow divides among multiple branches (e.g., Lister, 1992).

5.1.3. Erosive-depositional features

The Pantelleria volcanic edifice is generally characterized by small-scale mass wasting features (i.e., landslide/erosive scars and underlying gullies), mostly affecting the edge of the insular shelf and overlying terraced features (Figs. 4, 6, 7, 8 and 12). Based on the morphological (Figs. 3–7) and seismic characteristics (inner prograding geometry in Fig. 7c), the terraced morphologies lying on the shelf have been interpreted as submarine depositional terraces (SDT), i.e., sandy bodies commonly found on insular shelves (e.g., Casalbore et al., 2017 and reference therein; Ricchi et al., 2018; Innocentini et al., 2022). Their genesis has been associated with the downward transport of sediments from the surf zone and shoreface during stormy conditions in sub-actual conditions (last 6–7 ka; Chiocci and Orlando, 1996; Hernández-Molina et al., 2000; Chiocci and Romagnoli, 2004). At Pantelleria, their formation can be attributed to the wave reworking of volcaniclastic sediments produced by erosion and entering the sea. The nearshore SDT (edge at 30–50 m depth) is almost continuous along most part of the island, especially in the southern sector, characterized by older and widely eroded units, with cliffs locally exceeding 200 m of elevation. Differently, the SDT is almost absent in the north-western area, characterized by low rocky shoreline, associated with recent volcanic progradation of lava flows.

The spatial distribution of small-scale mass wasting features is similar to what was reported for other insular volcanoes (Romagnoli et al., 2013; Casalbore et al., 2018; Quartau et al., 2018; Ricchi et al., 2020; Chang et al., 2021), evidencing how the shelf and SDT edges are susceptible areas for mass-wasting processes. This is probably due to the marked increase in slope gradients below these edges (Fig. 2b) where the foreset of prograding bodies, made up of non-cohesive sediment, are at or close to their resting angle, so that they can be easily remobilized by different triggering mechanisms, such as eruptive or seismic shacking or cyclic loading due to storm-waves (especially in the case of near-shore SDTs). The steep and narrow gullies observed in shallow-water, sometimes merge downslope in larger channelized features. These channels are rarely associated with main subaerial valleys or rivers, indicating a main role played by marine retrogressive erosion in their formation. Their location is often controlled by lateral variations in the insular shelf morphology (i.e., width and edge depth), as for instance observed for Ch 3 and 5 in the SW sector or Ch 6 in the NE sector (Figs. 3, 4 and 7), possibly related to limits between sectors characterized by different age or lithologies.

In other cases, the development of channels is related to the distribution of volcanic features that create bathymetric lows on the submarine flanks, where sedimentary gravity flows can be channelized, such as for Ch 8 in the NW flank (Fig. 10). This channel's floor is characterized by arcuate or crescent-shaped bedforms, similar to those commonly observed in active canyons/channels along the submarine flanks of insular volcanoes (Casalbore et al., 2021 and reference therein; Chang et al., 2022), where they have been interpreted as upper-flow regime bedforms. The downslope change in crestline morphology of the bedforms (i.e., from arcuate and concave seawards to more sinuous and convex-seawards) can be referred to the marked decrease in slope gradient of the submarine flank, with the formation of unchannelized flows and fan-shaped deposits at its base. No landslide deposits are observed along the submarine part of Pantelleria, except for the deposits with blocky morphology recognized in proximity of the previous fan-shaped feature (Figs. 10, section BP3, and 12), indicating that this area has been affected by multiple mass-wasting processes during its recent evolution.

Erosive-depositional features are also concentrated on the North Valley, where erosive scars, crescent-shaped bedforms and enclosed depressions are recognizable (Figs. 2a, 9a and 12). All these features are oriented parallel to the isobaths suggesting the role of gravity-driven processes for their formation. This bathy-morphological setting is different from what observed in the Southern Valley, where a more subdued and smooth seafloor morphology is present (Fig. 2a). A tentative explanation for the uneven morphology of the NV floor could be related to the violent GT eruption occurred ~45 ka BP (Fig. 1b; section 2) and to the preferential distribution of related products in nearby marine areas. As reported by Anastasakis and Pe-Piper (2006), a 30-m long piston core LC-08 in the Pantelleria Basin (location in Fig. 1a) recovered 18 m of volcaniclastic deposits associated with energetic hyperconcentrated flows and diluted turbidity flows, correlated by the Authors to the GT eruption. These volcaniclastic deposits are overlain by 10 m of marly hemipelagic sediments, which correspond to an upper seismic unit (see Fig. 11 of Reeder et al., 2002) that can be correlated to the hemipelagic drape recognized in our seismic profiles (Fig. 9). Accordingly, the high-amplitude and irregular reflection at the base of the hemipelagic drape could represent the top of the GT-relate marine unit, also recognized in the downslope Pantelleria basin and retrieved in core LC-08. In this regard, coarse-grained volcanogenic deposits recovered in a gravity core performed on the northern flank of the NV (Romagnoli et al., 2024) were considered to represent the near-vent, primary marine equivalent of the distal Y-6 tephra layer, related to the ~45 ka old co-ignimbrite fallout deposit of the Green Tuff event. Other processes might have also played a role in the formation/reworking of erosive-depositional features observed in the NV. For instance, the formation/preservation of enclosed depressions (DEP in Figs. 7 and 9) could be explained by the interaction of an irregular subseafloor topography with the action of recent mass-wasting processes or bottom currents. Seismic profiles show that the observed hemipelagic drape is characterized by lateral and downslope variations in thickness, with the possible occurrence of a small contourite drift along the southern base of the Adventure bank slope (Fig. 9d). The key role played by bottom currents in the area is also testified the recognition of other contourite deposits identified both to the south by Reeder et al. (2002) and to the northwest of the PB by Martorelli et al. (2011). Considering the depth range of the NV (around 700–1200 m wd), we can also hypothesize a main role of the colder and denser, westward-flowing transitional Eastern Mediterranean Deep Water in the recent sedimentation.

5.2. Spatial and temporal evolution of the Pantelleria edifice

As discussed above, the morphological asymmetry of the Pantelleria volcanic edifice can be related to the main structural features of the Sicily Channel (Civile et al., 2008; Catalano et al., 2009) and to the interplay with volcanism and other processes. Along the main SE-NW oriented axis, marked morphological differences are recognizable between the different submarine parts of the volcano. In general, the SE flank is widely affected by erosional processes, appearing more degraded than the NW flank, and this fact may be explained by the overall NW migration of magmatic activity, also inferred through multichannel seismic reflection profiles in the Pantelleria basin (Civile et al., 2010). Therefore, an older age can be supposed for the south-eastern part of the volcano, where primary volcanic features are mostly smoothed by a relevant sedimentary drape (Fig. 3). A completely different setting appears for the NW submarine flank, where the field of volcanic cones and the elongated ridges are mostly characterized by a fresh and well-preserved morphology (Fig. 10), pointing to their likely younger age. It is worth mentioning that the last historical eruption of Pantelleria (i.e., the 1891 event; Conte et al., 2014; Kelly et al., 2014) occurred there. A quite similar trend of morphological differences in the submarine flanks has been recently depicted also for the nearby Linosa

volcanic edifice (southern Sicily Channel; Fig. 1a), and accordingly interpreted as the result of an overall SE-NW migration of volcanic activity over time (Romagnoli et al., 2020).

However, these findings are apparently in contrast with the notable width of the insular shelf in the NW flank with respect to the SE one (Figs. 2, 3, 5 and 10). The shelf extension, in fact, is commonly interpreted as a proxy for relative age reconstructions of volcanic edifices, by assuming that it reflects the cumulated erosive action of waves over different eustatic cycles, so that the width commonly increases with the edifice age (i.e., Menard, 1983; Quartau et al., 2010 and 2014; Romagnoli, 2013). Local deviations from this shelf width/age relationship have been observed among shelf sectors of the same age, but experiencing different controlling factors, such as the exposure of related coastal sectors to different wave regimes, difference in lithologies and resistance to erosion, tectonics, shelf infilling or subsequent mass-wasting processes (e.g., Quartau et al., 2010; Ramalho et al., 2013; Casalbore et al., 2015; Romagnoli et al., 2018). None of these factors seems to be appropriate to explain the large differences observed in the shelf in the study area; an hypothesis on its genesis is discussed further on, also considering information derived from another morphological parameter, i.e. the depth of the shelf edge.

5.2.1. *Sea level indicators and vertical mobility*

The depth of erosive shelf edge has been considered a marker of paleo sea-levels and it can be used to assess the vertical behaviour of volcanic flanks (Quartau et al., 2014; Lucchi et al., 2019). At Pantelleria, morpho-bathymetric data show an inverse (and contradictory) relationship between shelf width and the edge depth on the SE and NW Pantelleria shelves. The shelf edge is markedly deeper (over 200 m wd) in the narrow SE shelf than in the wider NW shelf (on average <130 m wd, green lines in Figs. 7 and 10), possibly indicating that differential vertical movements affected these areas after the shelf formation. The depth of the NW and NE shelf edge is comparable with the sea level reached during Pleistocene sea-level lowstands (Rohling et al., 2014) and is in agreement with the estimated value of 127 m wd for paleo sea level during the Last Glacial Maximum (LGM, ~20 ka) in the area obtained through glacio-hydro-isostatic modelling (Lambeck et al., 2011). This has two implications: 1) the entire NW shelf area was formed/reworked/rejuvenated at the time of the LGM and later on, and 2) this sector has been vertically stable, or just slight uplifted in the last 20 ka. Recent uplift processes along the N and (mostly) NE coastal sectors of Pantelleria Island are testified by three raised paleo-shorelines (max height 4.2 m) dated at 900 years ago, providing uplift rates up to 5 mm/yr centred on the Cala del Gadir (Fig. 1b; De Guidi and Monaco, 2009), as well as by historical records in the months immediately before the 1891 eruption, when a maximum uplift value of 1.0 m was measured along the NE coast (Riccò, 1892), but these rates refer to short-term, co-eruptive events. Differently, the deeper edge observed in the SE shelf implies (at least) 80 m of subsidence, which should be associated with long-term volcano-tectonic processes that affected this flank after the shelf formation, similarly to what recently proposed for the oldest sectors of Salina insular shelf in the Aeolian Islands (Lucchi et al., 2019). The similarity between the two case-studies is also reflected by the shelf morphology, showing a gently sloping (2–4°) sector down to 110–120 m wd, followed by a steeper sector (slope gradients of 15–20°) down to 200–220 m wd, just above the main break-in-slope (declivities >30°) with the underlying volcanic flank. This shelf setting can be explained considering that the shallower and gently sloping shelf sector was the seat of subaerial and marine erosion (and later deposition of SDTs) during the last eustatic hemicycle (after the LGM), while the deeper and steeper shelf was carved during the previous eustatic cycle(s), thus representing a paleo shelf-break and supporting a polygenic origin for this shelf sector. This also suggests that subsidence should have been relatively fast because the deeper carved shelf is very steep and narrow and did not have time to develop as a low-gradient surface.

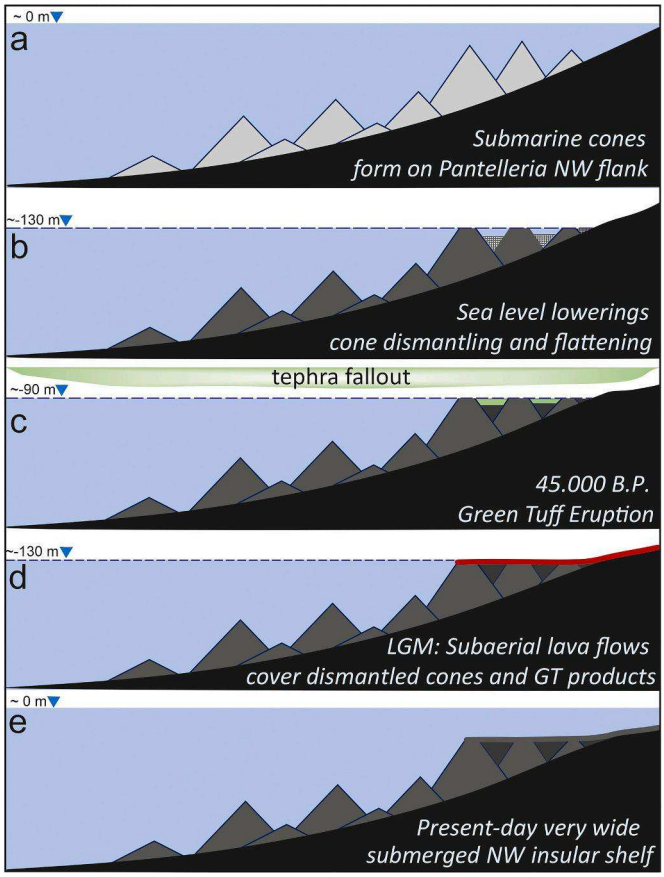

Fig. 13. Simplified sketch showing the formation of the wide NW insular shelf off Pantelleria island due to the interplay between volcanic and erosive-depositional processes associated modulated by sea level changes (the approximate sea level for each stage is reported on the left; 0 is referred to the present-day condition). The submarine cones present on the shallow-water portion of the NW flank of the Pantelleria (a) were partially dismantled and flattened by wave action during Late-Quaternary sea level fluctuations (b). The bathymetric lows among the volcanic cones were filled both by the eroded material (polygon with circles) and the large amount of volcaniclastic material (green polygon) emitted during the Green Tuff eruption at 45 ka BP (c). During the Last Glacial Maximum (LGM), basaltic effusive activity covered the shelf with the stacking of multiple lava flows (thick red line), leading to the rejuvenation of the insular shelf (d), then the sea level has reached its present-day level (e). (For interpretation of the references to colour in this figure legend, the reader is referred to the web version of this article.)

5.2.2. *Model of formation of the NW shelf*

If the younger age of the NW part of the island is supported by the fresh-looking volcanic morphologies, the occurrence of recent eruptive activity and the shallow depth of the shelf edge, we still have to reconcile these findings with the "anomalous" shelf width in this area (>4 km; Fig. 10).We propose a two-stage model to explain the formation of this shelf sector trough the interplay among submarine volcanic processes and Pleistocene sea level changes, in a context of migrating eruptive activity.

During an earlier stage, the formation of the shelf through erosive-depositional processes (mainly wave-erosion, considering the exposition to the most frequent and energetic storms coming from NW sectors), modulated by Late-Quaternary Sea level fluctuations, would have dismantled the volcanic products that at that time formed the shallow-water NW sector of the Pantelleria volcanic edifice (Figs. 13 a and b). These products might represent the extension towards the island of the observed offshore field of volcanic cones, as supported by the truncation of some of these cones close to the NW outer shelf (see red arrows in Fig. 10c) as well as by the remnants of two eroded volcanic centres on

the shelf surface (EVC in Fig. 10). The proposed model of a progressive shelf enlargement due to the wave-erosion of shallow-water submarine volcanic cones (located close to the island) during eustatic cycles is also suggested by the comparison with the present-day setting of the NW shelf of the nearby Linosa Island (also located in the Sicily Channel, Fig. 1a). At Linosa, the NW insular shelf is coalescent with a volcanic cone (Secca Maestra; Romagnoli et al., 2020) similar in shape and size to those observed in the NW offshore of Pantelleria. The summit of this pointy cone is located at ~40 m wd, indicating a relatively young age for this cone, since otherwise it would have been dismantled by wave erosion during the last hemieustatic cycle. In the case of future lowering of the sea level, the upper part of this cone would be dismantled by wave erosion, leading to a further enlargement of the present-day insular shelf there.

At Pantelleria, it should be considered that the eroded, shallow-water volcanic centres located in the NW sector could have been covered by the emplacement of the large amount of volcanic material emitted during the Green Tuff eruption at ~45 ka (Fig. 13c), that overlain large part of the island with maximum thickness of 20 m (Rotolo et al., 2017 and reference therein). It is thus reasonable to assume that, being deposited during the last sea level lowering (around stage MIS3a, when the coastline was in mid-shelf position between 65 and 100 m wd), the GT units were deposited here in a partially subaerial environment, filling the depressed area between volcanic centres, and may have been easily re-mobilized by the subsequent falling sea level, contributing to the development of an overall gently sloping shelf surface before or during the last sea level fall culminated at 20 ka BP.

In a later stage, during the last hemieustatic cycle, this earlier shelf would have been rejuvenated (sensu Quartau et al., 2015) by the products of effusive basaltic activity emitted in this area between 29 ka (Fig. 13d) and 10 ka, as suggested by the morphological steps recognizable on the NW shelf down to 130 m wd (MS in Fig. 10). These steps can be interpreted, in fact, as the frontal edge of lava flows and/or paleo-shorelines, formed and partially reworked during the LGM and successive sea level rise (Calarco, 2011). The progradation of these lava fronts would have resulted in a significant shallowing of the shelf edge, as also evidenced by the local remnant of a deeper and "not rejuvenated" shelf edge segment around ~160 m wd (orange line in Fig. 10a).

A recent example of shelf rejuvenation can be recognized on the NE shelf (Fig. 7), where the Khaggiar lava flows, emitted at ~5 ka (Rotolo et al., 2021 and reference therein), extend 2.5 km away from the source vent, prograding over the previously formed insular shelf and totally covering it. The shelf is, instead, clearly recognizable in the surrounding sectors (by comparison of sections BP1 and BP2 in Fig. 7). The marine sector off Khaggiar is instead characterized by a very narrow coastal platform (CP in Fig. 7), whose shallow edge depth (15–25 m wd) is comparable with similar wave-cut features related to the present-day sea level conditions in the Mediterranean Sea, such as the recent Vulcanello lava platform in the Aeolian Islands (Romagnoli et al., 2012; Casalbore et al., 2019). This inference supports our model that the progradation of lava flows on the NW shelf of Pantelleria should have contributed to its enlargement and shallowing.

6. Conclusions

The integrated analysis of multibeam bathymetry and seismic data allowed us to constrain the interplay among volcanic, tectonic and erosive-depositional processes in controlling the morphological evolution of Pantelleria volcano. The interaction between volcanic and tectonic processes is recognizable at different spatial and time scales, from the marked asymmetry of the entire volcano development along the SE-NW direction to the preferential elongation/alignment of volcanic cones, ridges and eruptive fissures along its flanks.

The marked difference between the more degraded and subdued volcanic morphologies recognizable on the SE submarine flank with respect to the fresh-looking volcanic field on the NW flank supports an overall migration from SE to NW over time, in agreement with the results of previous studies. However, this migration is seemingly in contrast with the development of a much wider (4 km) and shallower (< 130 m wd) NW insular shelf, with respect to the 2-km wide and deep (edge at 210 m wd) SE shelf. This setting can be explained by interpreting the NW shelf as a polygenic feature, formed in two main stages, modulated by Pleistocene sea level fluctuations, and involving the shelf rejuvenation due to the emplacement of later lava flows. This led to a marked shallowing of the NW shelf edge at water depths comparable to those reached by the sea level during the LGM, i.e. around 130 m wd. Shelf edges lying at similar or shallower depths are observed along most part of the NE and SW flank, indicating an overall vertical stability or uplift since the LGM. Differently, the deeper paleo shelf edge identified on the SE submerged flank indicates that this sector was affected by a significant subsidence of (at least) 80 m after the shelf formation.

The recent/present-day wave base-level controlled the formation, around the island, of an almost continuous near-shore submarine depositional terrace, except off the NW sector (mainly due to recent emplacement of lava flows here), in relation to wave reworking of volcaniclastic sediments in the coastal area. At the edge of this depositional terrace and at the shelf edge, small-scale mass wasting processes produce erosive features that, locally, lead to the development of main channels along the submarine flanks and to the transfer of sediments to deeper water.

More generally, this study highlights the key role played by morpho-stratigraphic studies for better understanding the volcano-tectonic evolution of insular and coastal volcanoes, also providing insights for reconstructing Late-Quaternary vertical movements typically affecting volcanic edifices.

Supplementary data to this article can be found online at https://doi.org/10.1016/j.margeo.2024.107308.

CRediT authorship contribution statement

Daniele Casalbore: Writing – original draft, Visualization, Investigation, Formal analysis, Data curation, Conceptualization. **Claudia Romagnoli:** Writing – original draft, Formal analysis. **Marilena Calarco:** Writing – original draft, Formal analysis. **Alessandro Bosman:** Writing – original draft, Formal analysis, Data curation. **Eleonora Martorelli:** Writing – original draft, Formal analysis. **Francesco Latino Chiocci:** Writing – original draft, Formal analysis.

Declaration of competing interest

The authors declare no conflict of interest.

Data availability

Multibeam data used for this work are downloadable from the EMODnet BATHYMETRY website (https://portal.emodnet-bathymetry.eu/). Multichannel seismic profiles from the Mediterranean Sea MS lines, also called Ministerial Seismic lines are downloadable from Videpi website (https://www.videpi.com/videpi/videpi.asp). The seismic data collected during the Panther Cruise are available in the Eurofleet Project website (https://www.eurofleets.eu/access/previous-calls/eurofleets2-regional-3-call-results/eurofleets2-funded-project-panther-results/) or upon request to the P.I. of the cruise Sara Benetti s.benetti@ulster.ac.uk.

Acknowledgements

The captains, crews and participants of the three cruises (two onboard R.V. Urania of the CNR and another onboard a small vessel for coastal survey for archeological purposes) are gratefully acknowledged. The Ministero dell'Ambiente e della Tutela del Territorio e del Mare-Geoportale Nazionale with license Creative Commons 3.0 Italy (CC BY-SA-3.0IT) is acknowledged for providing the terrestrial LIDAR data.

We also thanks the European Union Seventh Framework Programme (FP7/2007-2013) under Grant Agreement n° 312762-EUROFLEETS2, project "PANTelleria High-energy ERuptions from marine studies (PANTHER)" (PI S. Benetti) for availability of the collected seismic data. The first author also thanks the funding provided by the "Progetto di Ateneo medio 2021 and 2022" (P·I Daniele Casalbore). The authors would like to thank Dr. Rui Quartau and Prof. Patrick Bachèlery for their useful suggestions that helped improving the quality of the paper.

References

Abelli, L., Agosto, M.V., Casalbore, D., Romagnoli, C., Bosman, A., Antonioli, F., Chiocci, F.L., 2016. Marine geological and archaeological evidence of a possible pre-Neolithic site in Pantelleria Island, Central Mediterranean Sea. Geol. Soc. Lond. Spec. Publ. 411 (1), 97–110.

Anastasakis, G., Pe-Piper, G., 2006. An 18 m thick volcaniclastic interval in Pantelleria Trough, Sicily Channel, deposited from a large gravitative flow during the Green Tuff eruption. Mar. Geol. 231 (1–4), 201–219.

Astraldi, M, Gasparini, GP, Gervasio, L, Salusti, E, 2001. Dense water dynamics along the Strait of Sicily (Mediterranean Sea). J. Phys. Oceanogr. 31, 3457–3475.

Boccaletti, M., Cello, G., Tortorici, L., 1987. Transtensional tectonics in the Sicily Channel. J. Struct. Geol. 9 (7), 869–876.

Bosman, A., Casalbore, D., Anzidei, M., Muccini, F., Carmisciano, C., Francesco Latino, C., 2015. The first ultra-high resolution Digital Terrain Model of the shallow-water sector around Lipari Island (Aeolian Islands, Italy). Ann. Geophys. 58, S0218.

Boudon, G., Le Friant, A., Komorowski, J.C., Deplus, C., Semet, M.P., 2007. Volcano flank instability in the Lesser Antilles Arc: diversity of scale, processes, and temporal recurrence. J. Geophys. Res. Solid Earth 112 (B8).

Briais, A., Sloan, H., Parson, L.M., Murton, B.J., 2000. Accretionary processes in the axial valley of the Mid-Atlantic Ridge 27 N–30 N from TOBI side-scan sonar images. Mar. Geophys. Res. 21, 87–119.

Calanchi, N., Colantoni, P., Rossi, P.L., Saitta, M., Serri, G., 1989. The Strait of Sicily continental rift systems: physiography and petrochemistry of the submarine volcanic centres. Mar. Geol. 87 (1), 55–83.

Calarco, M., 2011. In: Unpublished Ph.D. Thesis (Ed.), Integrated analyses of the submarine volcanic structures offshore Pantelleria, p. 195.

Carey, S., 2000. Volcaniclastic sedimentation around island arcs. In: Sigurdsson, H. (Ed.), Encyclopedia of Volcanoes. Academic Press, San Diego, pp. 627–642.

Carillo, A., Bargagli, A., Caiaffa, E., Iacono, R., Sannino, G., 2012. Stima del Potenziale Energetico Associato al Moto Ondoso in Regioni Campione della Costa Italiana. Available online: http://openarchive.enea.it/handle/10840/4525 (accessed on 3 August 2016).

Carracedo, J.C., Troll, V.R., Zaczek, K., Rodríguez-González, A., Soler, V., Deegan, F.M., 2015. The 2011–2012 submarine eruption off El Hierro, Canary Islands: new lessons in oceanic island growth and volcanic crisis management. Earth Sci. Rev. 150, 168–200.

Casalbore, D., 2018. Volcanic islands and seamounts. Submarine Geomorphol. 333–347.

Casalbore, D., Ridente, D., Bosman, A., Chiocci, F., 2011. The Italian MaGIC project. Hydro Int. 24–27.

Casalbore, D., Romagnoli, C., Pimentel, A., Quartau, R., Casas, D., Ercilla, G., Chiocci, F. L., 2015. Volcanic, tectonic and mass-wasting processes offshore Terceira Island (Azores) revealed by high-resolution seafloor mapping. Bull. Volcanol. 77, 1–19.

Casalbore, D., Bosman, A., Romagnoli, C., Di Filippo, M., Chiocci, F.L., 2016. Morphology of Lipari offshore (Southern Tyrrhenian Sea). J. Maps 12 (1), 77–86.

Casalbore, D., Falese, F., Martorelli, E., Romagnoli, C., Chiocci, F.L., 2017. Submarine depositional terraces in the Tyrrhenian Sea as a proxy for paleo-sea level reconstruction: Problems and perspective. Quat. Int. 439, 169–180.

Casalbore, D., Romagnoli, C., Bosman, A., Anzidei, M., Chiocci, F.L., 2018. Coastal hazard due to submarine canyons in active insular volcanoes: examples from Lipari Island (southern Tyrrhenian Sea). J. Coast. Conserv. 22, 989–999.

Casalbore, D., Romagnoli, C., Bosman, A., De Astis, G., Lucchi, F., Tranne, C.A., Chiocci, F.L., 2019. Multi-stage formation of La Fossa Caldera (Vulcano Island, Italy) from an integrated subaerial and submarine analysis. Mar. Geophys. Res. 40, 479–492.

Casalbore, D., Clare, M.A., Pope, E.L., Quartau, R., Bosman, A., Chiocci, F.L., Santos, R., 2021. Bedforms on the submarine flanks of insular volcanoes: new insights gained from high resolution seafloor surveys. Sedimentology 68 (4), 1400–1438.

Casas, D., Pimentel, A., Pacheco, J., Martorelli, E., Sposato, A., Ercilla, G., Chiocci, F., 2018. Serreta 1998–2001 submarine volcanic eruption, offshore Terceira (Azores): characterization of the vent and inferences about the eruptive dynamics. J. Volcanol. Geotherm. Res. 356, 127–140.

Catalano, S., De Guidi, G., Lanzafame, G., Monaco, C., Tortorici, L., 2009. Late Quaternary deformation on the island on Pantelleria: new constraints for the recent tectonic evolution of the Sicily Channel Rift (southern Italy). J. Geodyn. 48 (2), 75–82.

Cavallaro, L., Iuppa, C., Castiglione, F., Musumeci, R.E., Foti, E., 2020. A simple model to assess the performance of an overtopping wave energy converter embedded in a port breakwater. J. Marine Sci. Eng. 8 (11), 858. https://doi.org/10.3390/jmse8110858.

Chang, Y.-C., Mitchell, N.C., Quartau, R., 2021. Landslides in the upper submarine slopes of volcanic islands: the central Azores. Geochem. Geophys. Geosyst. 22, e2021GC009833.

Chang, Y.-C., Mitchell, N.C., Quartau, R., Hubscher, C., Rusu, L., Tempera, F., 2022. Asymmetric abundances of submarine sediment waves around the Azores volcanic islands. Mar. Geol. 449 (106), 837.

Chiocci, F.L., Casalbore, D., 2017. Unexpected fast rate of morphological evolution of geologically-active continental margins during Quaternary: examples from selected areas in the Italian seas. Mar. Pet. Geol. 82, 154–162.

Chiocci, F.L., Orlando, L., 1996. Lowstand terraces on Tyrrhenian Sea steep continental slopes. Mar. Geol. 134 (1–2), 127–143.

Chiocci, F.L., Romagnoli, C., 2004. Submerged depositional terraces in the Aeolian Islands (Sicily). In: Chiocci, F.L., D'Angelo, S., Romagnoli, C. (Eds.), Atlas of Submerged Depositional Terraces Along the Italian Coasts, Memorie Descrittive della Carta Geologica d'Italia. Agenzia per la Protezione dell' Ambiente e per i Servizi Tecnici (APAT), Roma, pp. 81–114.

Civetta, L., Cornette, Y., Crisci, G., Gillot, P.Y., Orsi, G., Requejo, C.S., 1984. Geology, geochronology and chemical evolution of the island of Pantelleria. Geol. Mag. 121 (6), 541–562.

Civetta, L., Cornette, Y., Gillot, P.Y., Orsi, G., 1988. The eruptive history of Pantelleria (Sicily Channel) in the last 50 ka. Bull. Volcanol. 50, 47–57.

Civile, D., Lodolo, E., Tortorici, L., Lanzafame, G., Brancolini, G., 2008. Relationships between magmatism and tectonics in a continental rift: the Pantelleria Island region (Sicily Channel, Italy). Mar. Geol. 251 (1–2), 32–46.

Civetta, L., Cornette, Y., Gillot, P.Y., Orsi, G., 1988. The eruptive history of Pantelleria (Sicily Channel) in the last 50 ka. Bull. Volcanol. 50, 47–57.

Civile, D., Lodolo, E., Accettella, D., Geletti, R., Ben-Avraham, Z., Deponte, M., Romeo, R., 2010. The Pantelleria graben (Sicily Channel, Central Mediterranean): an example of intraplate 'passive'rift. Tectonophysics 490 (3–4), 173–183.

Clare, M.A., Yeo, I.A., Watson, S., Wysoczanski, R., Seabrook, S., Mackay, K., Williams, M., 2023. Fast and destructive density currents created by ocean-entering volcanic eruptions. Science 381 (6662), 1085–1092.

Colombier, M., Scheu, B., Wadsworth, F.B., Cronin, S., Vasseur, J., Dobson, K.J., et al., 2018. Vesiculation and quenching during surtseyan eruptions at hunga tonga-hunga ha'apai volcano, tonga. J. Geophys. Res. Solid Earth 123 (5), 3762–3779. https://doi.org/10.1029/2017JB015357.

Conte, A.M., Martorelli, E., Calarco, M., Sposato, A., Perinelli, C., Coltelli, M., Chiocci, F. L., 2014. The 1891 submarine eruption offshore Pantelleria Island (Sicily Channel, Italy): Identification of the vent and characterization of products and eruptive style. Geochem. Geophys. Geosyst. 15 (6), 2555–2574.

Coombs, M., Wallace, K., Cameron, C., Lyons, J., Wech, A., Angeli, K., Cervelli, P., 2019. Overview, chronology, and impacts of the 2016–2017 eruption of Bogoslof volcano, Alaska. Bull. Volcanol. 81 (11), 62. https://doi.org/10.1007/s00445-019-1322-9.

Corazzato, C., Tibaldi, A., 2006. Fracture control on type, morphology and distribution of parasitic volcanic cones: an example from Mt. Etna, Italy. J. Volcanol. Geotherm. Res. 158 (1–2), 177–194.

Corti, G., Cuffaro, M., Doglioni, C., Innocenti, F., Manetti, P., 2006. Coexisting geodynamic processes in the Sicily Channel. Geol. Soc. Am. Spec. Pap. 409, 83–96.

De Guidi, G., Monaco, C., 2009. Late Holocene vertical deformation along the coast of Pantelleria Island (Sicily Channel, Italy). Quat. Int. 206 (1–2), 158–165.

Dietterich, H.R., Cashman, K.V., 2014. Channel networks within lava flows: Formation, evolution, and implications for flow behavior. J. Geophys. Res. Earth Surf. 119 (8), 1704–1724.

Embley, R.W., Tamura, Y., Merle, S.G., Sato, T., Ishizuka, O., Chadwick Jr., W.W., Wiens, D.A., Shore, P., Stern, R.J., 2014. Eruption of South Sarigan Seamount, Northern Mariana Islands: Insights into hazards from submarine volcanic eruptions. Oceanography 27 (2), 24–31.

Fialko, Y.A., Rubin, A.M., 1999. Thermal and mechanical aspects of magma emplacement in giant dike swarms. J. Geophys. Res. Solid Earth 104 (B10), 23,033–23,049.

Finetti, I., 1984. Geophysical study of the Sicily Channel rift zone. Boll. Geofis. Teor. Appl. 26, 3–28.

Fornaciai, A., Favalli, M., Karátson, D., Tarquini, S., Boschi, E., 2012. Morphometry of scoria cones, and their relation to geodynamic setting: a DEM-based analysis. J. Volcanol. Geotherm. Res. 217–218, 56–72.

Fulignati, P., Malfitano, G., Sbrana, A., 1997. The Pantelleria caldera geothermal system: data from the hydrothermal minerals. J. Volcanol. Geotherm. Res. 75 (3–4), 251–270.

Gaspar, J.L., Queiroz, G., Pacheco, J.M., Ferreira, T., Wallenstein, N., Almeida, M.H., Coutinho, R., 2003. Basaltic lava balloons produced during the 1998–2001 Serreta Submarine ridge eruption (Azores). In: White, J.D.L., et al. (Eds.), Explosive Subaqueous Volcanism. AGU, Washington, D. C., pp. 205–212

Giuffrida, M., Nicotra, E., Viccaro, M., 2020. Changing modes and rates of mafic magma supply at Pantelleria (Sicily Channel, Southern Italy): new perspectives on the volcano factory drawn upon olivine records. J. Petrol. 61 (5), egaa051.

Gregg, T.K., Smith, D.K., 2003. Volcanic investigations of the Puna Ridge, Hawai' i: relations of lava flow morphologies and underlying slopes. J. Volcanol. Geotherm. Res. 126 (1–2), 63–77.

Gregg, T.K.P., Fink, J.H., 1995. Quantification of submarine lava-flow morphology through analog experiments. Geology 23, 73–76.

Gregg, T.K.P., Fink, J.H., 2000. A laboratory investigation into the effects of slope on lava flow morphology. J. Volcanol. Geotherm. Res. 96 (3–4), 145–159.

Gudmundsson, A., 1986. Mechanical aspects of postglacial volcanism and tectonics of the Reykjanes Peninsula, southwest Iceland. J. Geophys. Res. Solid Earth 91 (B12), 12,711–12,721.

Harris, A.J., Flynn, L.P., Matias, O., Rose, W.I., Cornejo, J., 2004. The evolution of an active silicic lava flow field: an ETM+ perspective. J. Volcanol. Geotherm. Res. 135 (1–2), 147–168.

Head, J.W., Wilson, L., Smith, D.K., 1996. Mid-ocean ridge eruptive vent morphology and substructure: Evidence for dike widths, eruption rates, and evolution of eruptions and axial volcanic ridges. J. Geophys. Res. Solid Earth 101 (B12), 28,265–28,280.
Hernández-Molina, F.J., Fernández-Salas, L.M., Lobo, F., Somoza, L., Díaz-del-Río, V., Alveirinho Dias, J.M., 2000. The infralittoral prograding wedge: a new large-scale progradational sedimentary body in shallow marine environments. Geo-Mar. Lett. 20, 109–117.
Hunt, J.E., Tappin, D.R., Watt, S.F.L., Susilohadi, S., Novellino, A., Ebmeier, S.K., Udrekh, U., 2021. Submarine landslide megablocks show half of Anak Krakatau island failed on December 22nd, 2018. Nat. Commun. 12 (1), 2827.
Ikegami, F., McPhie, J., Carey, R., Mundana, R., Soule, A., Jutzeler, M., 2018. The eruption of submarine rhyolite lavas and domes in the deep ocean–Havre 2012, Kermadec Arc. Front. Earth Sci. 6, 147.
Innocentini, S., Quartau, R., Casalbore, D., Roque, C., Vinhas, A., Santos, R., Rodrigues, A., 2022. Morpho-stratigraphic characterization of the southern shelf of Porto Santo Island (Madeira Archipelago): insights for small-scale instability processes and post-LGM sedimentary architecture. Mar. Geol. 444 (106), 729.
Jordan, N.J., Rotolo, S.G., Williams, R., Speranza, F., McIntosh, W.C., Branney, M.J., Scaillet, S., 2018. Explosive eruptive history of Pantelleria, Italy: Repeated caldera collapse and ignimbrite emplacement at a peralkaline volcano. J. Volcanol. Geotherm. Res. 349, 47–73.
Kelly, J.T., Carey, S., Pistolesi, M., Rosi, M., Croff-Bell, K.L., Roman, C., Marani, M., 2014. Exploration of the 1891 Foerstner submarine vent site (Pantelleria, Italy): insights into the formation of basaltic balloons. Bull. Volcanol. 76, 1–18.
Lambeck, K., Antonioli, F., Anzidei, M., Ferranti, L., Leoni, G., Scicchitano, G., Silenzi, S., 2011. Sea level change along the Italian coast during the Holocene and projections for the future. Quat. Int. 232 (1–2), 250–257.
Lister, J.R., 1992. Viscous flows down and inclined plane from point and line sources. J. Fluid Mech. 242, 631–653.
Lucchi, F., Ricchi, A., Romagnoli, C., Casalbore, D., Quartau, R., 2019. Late Quaternary paleo sea level geomorphological markers of opposite vertical movements at Salina volcanic island (Aeolian Arc). Earth Surf. Process. Landf. 44 (12), 2377–2395.
Lynett, P., McCann, M., Zhou, Z., Renteria, W., Borrero, J., Greer, D., Cinar, G.E., 2022. Diverse tsunamigenesis triggered by the Hunga Tonga-Hunga Ha'apai eruption. Nature 609 (7928), 728–733.
Mahood, G.A., Hildreth, W., 1986. Geology of the peralkaline volcano at Pantelleria, Strait of Sicily. Bull. Volcanol. 48, 143–172.
Maiorana, M., Artoni, A., Le Breton, E., Sulli, A., Chizzini, N., Torelli, L., 2023. Is the Sicily Channel a simple Rifting Zone? New evidence from seismic analysis with geodynamic implications. Tectonophysics 864 (230), 019.
Martorelli, E., Petroni, G., Chiocci, F.L., Pantelleria Scientific Party, 2011. Contourites offshore Pantelleria Island (Sicily Channel, Mediterranean Sea): depositional, erosional and biogenic elements. Geo-Mar. Lett. 31, 481–493.
Menard, H.W., 1983. Insular erosion, isostasy, and subsidence. Science 220 (4600), 913–918.
Minami, H., Saitou, K., Ohara, Y., 2022. The Amami Rift: clarifying the roles of rifting and volcanism in the central Ryukyu Arc. Mar. Geol. 450 (106), 839.
Mitchell, N.C., 2003. Susceptibility of mid-ocean ridge volcanic islands and seamounts to large-scale landsliding. J. Geophys. Res. Solid Earth 108 (B8).
Mitchell, N.C., Masson, D.G., Watts, A.B., Gee, M.J., Urgeles, R., 2002. The morphology of the submarine flanks of volcanic ocean islands: a comparative study of the Canary and Hawaiian hotspot islands. J. Volcanol. Geotherm. Res. 115 (1–2), 83–107.
Orsi, G., Gallo, G., Zanchi, A., 1991. Simple-shearing block resurgence in caldera depressions. A model from Pantelleria and Ischia. J. Volcanol. Geotherm. Res. 47 (1–2), 1–11.
Quartau, R., Trenhaile, A.S., Mitchell, N.C., Tempera, F., 2010. Development of volcanic insular shelves: Insights from observations and modelling of Faial Island in the Azores Archipelago. Mar. Geol. 275 (1–4), 66–83.
Quartau, R., Hipólito, A., Romagnoli, C., Casalbore, D., Madeira, J., Tempera, F., Chiocci, F.L., 2014. The morphology of insular shelves as a key for understanding the geological evolution of volcanic islands: insights from Terceira Island (Azores). Geochem. Geophys. Geosyst. 15 (5), 1801–1826.
Quartau, R., Madeira, J., Mitchell, N.C., Tempera, F., Silva, P.F., Brandão, F., 2015. The insular shelves of the Faial-Pico Ridge (A zores archipelago): a morphological record of its evolution. Geochem. Geophys. Geosyst. 16 (5), 1401–1420.
Quartau, R., Ramalho, R.S., Madeira, J., Santos, R., Rodrigues, A., Roque, C., Carrara, G., Brum da Silveira, A., 2018. Gravitational, erosional and depositional processes on volcanic ocean islands: insights from the submarine morphology of Madeira archipelago. Earth Planet. Sci. Lett. 482, 288–299.
Ramalho, R.S., Quartau, R., Trenhaile, A.S., Mitchell, N.C., Woodroffe, C.D., Ávila, S.P., 2013. Coastal evolution on volcanic oceanic islands: a complex interplay between volcanism, erosion, sedimentation, sea-level change and biogenic production. Earth-Sci. Rev. 127, 140–170.
Reeder, M.S., Rothwell, G., Stow, D.A., 2002. The Sicilian gateway: anatomy of the deep-water connection between East and West Mediterranean basins. Geol. Soc. Lond. Mem. 22, 171–189.
Ricchi, A., Quartau, R., Ramalho, R.S., Romagnoli, C., Casalbore, D., da Cruz, J.V., Vinhas, A., 2018. Marine terrace development on reefless volcanic islands: New insights from high-resolution marine geophysical data offshore Santa Maria Island (Azores Archipelago). Mar. Geol. 406, 42–56.
Ricchi, A., Quartau, R., Ramalho, R.S., Romagnoli, C., Casalbore, D., Zhao, Z., 2020. Imprints of volcanic, erosional, depositional, tectonic and mass-wasting processes in the morphology of Santa Maria insular shelf (Azores). Mar. Geol. 424 (106), 163.
Riccò, A., 1892. Terremoti sollevamento ed. eruzione sottomarina a Pantelleria nella seconda metà dell'Ottobre 1891. Boll. Soc. Geol. Ital. 130–156.
Rohling, E.J., Foster, G.L., Grant, K.M., Marino, G., Roberts, A.P., Tamisiea, M.E., Williams, F., 2014. Sea-level and deep-sea-temperature variability over the past 5.3 million years. Nature 508 (7497), 477–482.
Romagnoli, C., 2013. Characteristics and morphological evolution of the Aeolian volcanoes from the study of submarine portions. In: Lucchi, F., Peccerillo, A., Keller, J., Tranne, C.A., Rossi, P.L. (Eds.), The Aeolian Islands Volcanoes, 37(1). Geological Society, London, Memoirs, pp. 13–26.
Romagnoli, C., Casalbore, D., Chiocci, F.L., Bosman, A., 2009. Offshore evidence of large-scale lateral collapses on the eastern flank of Stromboli, Italy, due to structurally-controlled, bilateral flank instability. Mar. Geol. 262 (1–4), 1–13.
Romagnoli, C., Casalbore, D., Chiocci, F.L., 2012. La Fossa Caldera breaching and submarine erosion (Vulcano island, Italy). Mar. Geol. 303, 87–98.
Romagnoli, C., Casalbore, D., Bortoluzzi, G., Bosman, A., Chiocci, F.L., D'oriano, F., Marani, M., 2013. Bathy-morphological setting of the Aeolian Islands. In: Lucchi, F., Peccerillo, A., Keller, J., Tranne, C.A., Rossi, P.L. (Eds.), The Aeolian Islands Volcanoes, 37(1). Geological Society, London, Memoirs, pp. 27–36.
Romagnoli, C., Casalbore, D., Ricchi, A., Lucchi, F., Quartau, R., Bosman, A., Chiocci, F. L., 2018. Morpho-bathymetric and seismo-stratigraphic analysis of the insular shelf of Salina (Aeolian archipelago) to unveil its Late-Quaternary geological evolution. Mar. Geol. 395, 133–151.
Romagnoli, C., Belvisi, V., Innangi, S., Di Martino, G., Tonielli, R., 2020. New insights on the evolution of the Linosa volcano (Sicily Channel) from the study of its submarine portions. Mar. Geol. 419 (106), 060.
Romagnoli, C., Giglio, C., Conte, A.M., Cloke-Hayes, A., Garcia, M., Gasparotto, G., Benetti, S., 2024. New evidence of the Green Tuff deposits and post-caldera, recent explosive volcanic activity at Pantelleria volcano (Sicily Channel, Italy) recorded in near-vent marine areas. J. Volcanol. Geotherm. Res. 446 (107), 997.
Rotolo, S.G., Scaillet, S., La Felice, S., Vita-Scaillet, G., 2013. A revision of the structure and stratigraphy of pre-Green Tuff ignimbrites at Pantelleria (Strait of Sicily). J. Volcanol. Geotherm. Res. 250, 61–74.
Rotolo, S.G., Agnesi, V., Conoscenti, C., Lanzo, G., 2017. Pantelleria Island (Strait of Sicily): volcanic history and geomorphological landscape. Landscapes Landforms Italy 479–487.
Rotolo, S.G., Scaillet, S., Speranza, F., White, J.C., Williams, R., Jordan, N.J., 2021. Volcanological evolution of Pantelleria Island (Strait of Sicily) peralkaline volcano: a review. Comptes Rendus. Géosci. 353 (S2), 111–132.
Sigurdsson, H., Houghton, B., McNutt, S., Rymer, H., Stix, J., 2000. Encyclopedia of Volcanoes. Academic Press, pp. 361–400.
Smith, D.K., Cann, J.R., 1993. Building the crust at the Mid-Atlantic Ridge. Nature 365 (6448), 707–715.
Somoza, L., González, F.J., Barker, S.J., Madureira, P., Medialdea, T., De Ignacio, C., Palomino, D., 2017. Evolution of submarine eruptive activity during the 2011–2012 E l Hierro event as documented by hydroacoustic images and remotely operated vehicle observations. Geochem. Geophys. Geosyst. 18 (8), 3109–3137.
Tzevahirtzian, A., Zaragosi, S., Bachèlery, P., Biscara, L., Marchès, E., 2021. Submarine morphology of the Comoros volcanic archipelago. Mar. Geol. 432 (106), 383.
Washington, H.S., 1909. ART. VIII.–The Submarine Eruptions of 1831 and 1891 near Pantelleria. Am. J. Sci. (1880–1910) 27 (158), 131.
Watts, A.B., Peirce, C., Grevemeyer, I., Paulatto, M., Stratford, W., Bassett, D., De Ronde, C.E.J., 2012. Rapid rates of growth and collapse of Monowai submarine volcano in the Kermadec Arc. Nat. Geosci. 5 (7), 510–515.
White, J.C., Parker, D.F., Ren, M., 2009. The origin of trachyte and pantellerite from Pantelleria, Italy: insights from major element, trace element, and thermodynamic modelling. J. Volcanol. Geotherm. Res. 179 (1–2), 33–55.
Wright, I.C., Chadwick Jr., W.W., de Ronde, C.E., Reymond, D., Hyvernaud, O., Gennerich, H.H., Bannister, S.C., 2008. Collapse and reconstruction of Monowai submarine volcano, Kermadec arc, 1998–2004. J. Geophys. Res. Solid Earth 113 (B8).
Zanchetta, G., Giaccio, B., Bini, M., Sarti, L., 2018. Tephrostratigraphy of Grotta del Cavallo, Southern Italy: insights on the chronology of Middle to Upper Palaeolithic transition in the Mediterranean. Quat. Sci. Rev. 182, 65–77.